

1 **Targeting of temperate phages drives loss of type I CRISPR-Cas**  
2 **systems**

3 Clare Rollie<sup>1,2\*</sup>, Anne Chevallereau<sup>1,2\*</sup>, Bridget N.J. Watson<sup>1</sup>, Te-yuan Chyou<sup>3</sup>, Olivier Fradet<sup>1</sup>,  
4 Isobel McLeod<sup>1</sup>, Peter C. Fineran<sup>4,5</sup>, Chris M. Brown<sup>3,5</sup>, Sylvain Gandon<sup>6</sup> and Edze R. Westra<sup>1\*</sup>

5

6 **Affiliations:**

7 <sup>1</sup>ESI, Biosciences, University of Exeter, Cornwall Campus, Penryn TR10 9EZ, UK.

8 <sup>2</sup>These authors contributed equally.

9 <sup>3</sup>Department of Biochemistry, University of Otago, Po Box 56, Dunedin 9054, New Zealand.

10 <sup>4</sup>Department of Microbiology and Immunology, University of Otago, Po Box 56, Dunedin 9054,  
11 New Zealand.

12 <sup>5</sup>Genetics Otago, University of Otago, Po Box 56, Dunedin 9054, New Zealand.

13 <sup>6</sup>CEFE UMR 5175, CNRS, Université de Montpellier, Université Paul-Valéry Montpellier,  
14 EPHE, 1919, Route de Mende, 34293 Montpellier Cedex 5, France

15

16 \*Correspondence to: C.Rollie@exeter.ac.uk ; A.Chevallereau@exeter.ac.uk ;  
17 E.R.Westra@exeter.ac.uk

18

1 **Upon infection of their host, temperate phages (viruses that infect bacteria) enter either**  
2 **a lytic or a lysogenic cycle. The former results in bacterial cell lysis and phage release**  
3 **(horizontal transmission), while lysogeny is characterized by integration of the phage**  
4 **in the host genome and dormancy (vertical transmission)<sup>1</sup>. Co-culture experiments of**  
5 **bacteria and temperate phage mutants, which are locked in the lytic cycle, have shown**  
6 **that CRISPR-Cas can efficiently eliminate the invading phages<sup>2,3</sup>. By contrast, here we**  
7 **show that when challenged with wild-type temperate phage that can become lysogenic,**  
8 **type I CRISPR-Cas immune systems are unable to eliminate these phages from the**  
9 **bacterial population. In fact, our data suggest that CRISPR-Cas immune systems are**  
10 **in this context maladaptive to the host due to severe immunopathological effects**  
11 **brought about by imperfect matching of spacers to integrated phage sequences**  
12 **(prophages). These fitness costs drive the loss of CRISPR-Cas from bacterial**  
13 **populations, unless the phage carries anti-CRISPR (*acr*) genes that suppress the**  
14 **immune system of the host. Using bioinformatics, we show that this imperfect targeting**  
15 **is likely to occur frequently in nature. These findings can help to explain the patchy**  
16 **distribution of CRISPR-Cas immune systems within and between bacterial species and**  
17 **highlight the strong selective benefits of phage-encoded *acr* genes for both the phage**  
18 **and host under these circumstances.**

19

20 CRISPR-Cas (Clustered Regularly Interspaced Short Palindromic Repeats; CRISPR-  
21 associated) adaptive immune systems provide sequence-specific resistance against phage  
22 infections by inserting phage-derived sequences (spacers) of around 30 bp into CRISPR loci  
23 on the host genome<sup>4</sup>. Upon reinfection, CRISPR transcripts guide Cas proteins to destroy the  
24 matching target<sup>5</sup>. The uptake of new spacers is far more efficient if a pre-existing spacer has  
25 partial complementarity to the phage. This process, known as “priming”, is widespread in type  
26 I systems, and provides protection against phage mutants that overcome host resistance by  
27 point mutation of their target sites<sup>6,7</sup>. However, partially matching spacers can also cause  
28 immunopathological effects when temperate phages enter the lysogenic lifecycle, where the

1 phage genome is integrated into that of the host and exists in a dormant state until it gets  
2 induced. Lysogeny is common but variable across bacterial genera<sup>8</sup>. During lysogeny, a  
3 primed CRISPR-Cas immune system may target the partially complementary site in the  
4 prophage, causing damage to both the phage and host DNA and resulting in induction of the  
5 SOS-response<sup>9</sup>. However, if and how these potentially negative effects impact the  
6 evolutionary and population dynamics of phage-bacteria interactions remains unclear, since  
7 these processes have only been studied in the context of virulent phages<sup>2,3</sup>.

8

### 9 **Temperate phages persist despite CRISPR**

10 To explore this, we infected *Pseudomonas aeruginosa* PA14 with either the temperate phage  
11 DMS3 or the virulent mutant DMS3*vir* (a DMS3 mutant that is locked in the lytic cycle through  
12 mutation of the c-repressor gene) and monitored bacterial and phage population dynamics for  
13 8 days. *P. aeruginosa* strain PA14 carries a type I-F CRISPR-Cas immune system, with spacer  
14 1 of CRISPR array 2 having an imperfect match (5 mismatches) to gene 42 of DMS3<sup>9,10</sup>. As  
15 previously reported<sup>3</sup>, DMS3*vir* was driven extinct by WT bacteria at 5 days post-infection (dpi)  
16 due to the evolution of CRISPR-based resistance, whereas a  $\Delta cas7$  mutant - lacking a  
17 functional CRISPR-Cas system - evolved surface-based resistance that allowed for phage  
18 persistence (Fig. 1a-c). In contrast, both WT and  $\Delta cas7$  bacteria were unable to clear wildtype  
19 DMS3 infections (Fig. 1b), suggesting that the ability to transmit vertically (i.e. lysogeny) is a  
20 critical determinant of temperate phage survival when bacteria encode CRISPR-Cas immune  
21 systems. To understand the evolutionary drivers of these population dynamics, we isolated  
22 bacterial clones from the DMS3-infected cultures at 3 dpi and quantified the proportion of  
23 lysogens and bacteria with CRISPR-based and surface-based resistance. This showed that  
24 CRISPR resistance evolution was significantly reduced in WT populations exposed to DMS3  
25 compared to DMS3*vir* (Fig. 1c,d), and instead many WT bacteria carried the DMS3 prophage  
26 (Fig. 1d), which confers phage resistance through superinfection exclusion. However,  
27 lysogeny levels were reduced in WT hosts compared to the  $\Delta cas7$  strain, which almost  
28 invariably carried the prophage (Fig. 1d).

1           The difference in DMS3 and DMS3*vir* persistence could be due to either differences in  
2 host resistance evolution or the ability of DMS3 to transmit vertically while continuously  
3 releasing free phage particles through prophage induction. To distinguish between these  
4 possibilities, we infected WT and  $\Delta cas7$  strains with an equal mix of DMS3 and DMS3*vir* and  
5 observed similar bacterial and phage population dynamics and resistance evolution to those  
6 during infection with temperate phage alone (Extended Data Fig. 1). Next, we examined how  
7 the relative frequencies of DMS3 and DMS3*vir* changed over time (Fig. 2a,b). Initially,  
8 DMS3*vir* outcompetes DMS3, consistent with the idea that high densities of sensitive hosts  
9 favour horizontal transmission (i.e. the lytic replication cycle)<sup>11</sup>. However, at later time points,  
10 all free phage particles belong to the DMS3 genotype. As the host population experienced by  
11 the two phage genotypes was identical, this demonstrates that vertical transmission facilitates  
12 the observed persistence of DMS3. Interestingly, persistence of free phages was facilitated  
13 despite low frequencies of lysogeny in WT compared to  $\Delta cas7$  bacteria (Fig. 2a,b, compare  
14 blue and red lines, and Extended Data Fig. 1c,d).

15           Next, to understand why lysogen formation was depressed in WT compared to  $\Delta cas7$   
16 bacteria, we performed temporal sampling of DMS3-infected populations over 7 days.  
17 Interestingly, this revealed that lysogeny in WT bacteria was already depressed at 1 dpi and  
18 continued to decline until 7 dpi, whereas the proportion of lysogens in isogenic mutants with  
19 a defective CRISPR-interference pathway ( $\Delta cas3$  and  $\Delta cas7$  mutants) was high and constant  
20 during this same period (Fig. 2c). Crucially, the proportion of DMS3 lysogens at 1 dpi was also  
21 depressed in a  $\Delta cas1$  mutant, which is unable to acquire novel spacers (adaptation) but is  
22 proficient in detecting and destroying complementary DNA (interference). However, in this  
23 background, the proportion of lysogens increased between 1 and 7 dpi to levels similar to the  
24 CRISPR-interference mutants (Fig. 2c). These data therefore suggest that WT and  $\Delta cas1$   
25 bacteria are partially resistant to DMS3 infection, even in the absence of spacer acquisition,  
26 resulting initially in fewer lysogens and further reductions if the hosts carry the genetic  
27 machinery to acquire additional spacers.

28

## 1 **Mismatched spacers are maladaptive**

2 We hypothesized that the observed suppression of lysogeny in WT and  $\Delta cas1$  backgrounds  
3 was dependent on the imperfect match (5 mismatches) between gene 42 of DMS3 and spacer  
4 1 of CRISPR array 2<sup>9,10</sup>. To test this, we infected a strain lacking CRISPR array 2 ( $\Delta CRISPR2$ )  
5 with DMS3 and observed that plasmid-based expression of spacer 1 ( $\Delta CRISPR2$ -sp1) led to  
6 similar population dynamics to those observed during infection of the wildtype strain (Extended  
7 Data Fig. 2a,b) and suppression of lysogeny (Extended Data Fig. 2c), while expression of a  
8 control non-targeting spacer ( $\Delta CRISPR2$ -NT) did not. To further corroborate the hypothesis  
9 that the suppression of lysogeny was caused by partial CRISPR-Cas resistance, we  
10 performed infections with phages carrying anti-CRISPR genes (*acr*), which are widespread  
11 and diverse genes (currently classified into 45 families) carried by a range of different mobile  
12 genetic elements, that block CRISPR-interference<sup>12</sup>. As expected, infection of WT bacteria  
13 with a mutant phage DMS3 carrying either *acrIF1* or *acrIF4*, both of which block the I-F  
14 CRISPR-Cas system of PA14<sup>13</sup>, showed similar lysogeny levels to those observed for  
15 interference-deficient mutants (Extended Data Fig. 3a).

16 Intriguingly, although lysogen formation was reduced in WT and  $\Delta cas1$  bacteria, the  
17 concentration of free phages was actually higher during the early stages of DMS3 infection of  
18 these hosts (Fig. 2d). This effect disappeared by 7 dpi - if bacteria were unable to acquire new  
19 spacers ( $\Delta cas1$ ) - or inverted at 4 dpi if they had a functional CRISPR-Cas system (Fig. 2d).  
20 This also coincided with reduced bacterial densities of WT and  $\Delta cas1$  populations compared  
21 to CRISPR-interference mutants during the early stages of the phage epidemic (Fig. 2e),  
22 suggesting that functional CRISPR-Cas immune systems may be maladaptive in this context.  
23 We speculated that the high DMS3 titres during early stages of infection of WT and  $\Delta cas1$   
24 bacteria (Fig. 2d and 1b) and the concurrent reduced bacterial densities could be due to  
25 interactions between the CRISPR interference machinery and the partially complementary  
26 prophage (i.e. autoimmunity), which can activate an SOS-response<sup>9</sup> and which in turn may  
27 trigger prophage induction<sup>14</sup>. To test this, we isolated 6 independent DMS3 lysogens from WT,  
28  $\Delta cas7$  and  $\Delta cas1$  backgrounds at 1 dpi. Growth measurements revealed significant fitness

1 costs of lysogeny in WT and  $\Delta cas1$  backgrounds, whereas growth of  $\Delta cas7$  lysogens was  
2 unaffected (Fig. 3a-c). Growth of lysogens lacking spacers 1 and 2 of CRISPR 2 ( $\Delta sp1-2$ ) or  
3 lacking the entire CRISPR 2 array ( $\Delta CRISPR2-NT$ ) was comparable to that of  $\Delta cas7$  lysogens  
4 (Fig. 3d and Extended Data Fig. 2c), but restoring the expression of CRISPR 2 spacer 1  
5 ( $\Delta CRISPR2-sp1$ ) resulted in a reduced growth rate (Extended Data Fig. 2d), confirming that  
6 this spacer is responsible for the reduced fitness of WT bacteria carrying the prophage.  
7 Competition of lysogens against bacteria with surface-based resistance confirmed a fitness  
8 cost of lysogeny in the WT, but not in the  $\Delta cas7$  background (Fig. 3e,f, relative fitness < 1, one-  
9 tailed Wilcoxon and t-tests, WT: df=5, p=0.016;  $\Delta cas7$ :  $t_5=3.6551$ , p=0.99). This effect was  
10 reduced if the prophage possessed an *acr* gene (Fig. 3e, one-tailed t-test, *acrIF1*:  $t_5=16.562$ ,  
11 *acrIF4*:  $t_5=14.805$  and p<0.0001 in both cases), whereas *acr* genes had no effect on fitness of  
12  $\Delta cas7$  lysogens (Fig. 3f, ANOVA  $F_{2,15}=0.205$ , p=0.82).

13         Next, we estimated prophage induction levels in WT and  $\Delta cas7$  lysogens. To this end,  
14 we pelleted bacterial cultures and washed away free phages, followed by resuspension in  
15 fresh medium, and monitored bacterial densities and free phage accumulation over 25 hours.  
16 While initial cell densities were similar for all strains, growth of WT cultures plateaued at a  
17 lower density (Extended Data Fig. 3b), yet they accumulated more phage particles compared  
18 to  $\Delta cas7$  lysogens (Extended Data Fig. 3c), unless the prophage carried an *acr* gene. Taken  
19 together, these data support the hypothesis that, unless DMS3 encodes *acr* genes, CRISPR-  
20 Cas causes immunopathology during vertical transmission of the phage, which triggers  
21 prophage induction and hence explains the high free phage titres during the early infection  
22 stage.

23         These immunopathological effects may select for CRISPR mechanisms that  
24 selectively target phages during their lytic cycle, as has been described for type III  
25 systems<sup>15,16</sup>. However, competition between DMS3 and DMS3*vir* phages showed that the  
26 main determinant of their relative fitness is the proportion of sensitive bacteria in the  
27 population<sup>11</sup> (Extended Data Fig. 3d, two-way ANOVA  $F_{6,83}=3.1683$ , p=0.008) and is  
28 independent of whether resistance of bacteria in the population was CRISPR-based or

1 surface-based (Extended Data Fig. 3d,  $F_{1,76}=2.8923$ ,  $p=0.09$ ). This suggests that the type I  
2 CRISPR-Cas system of *P. aeruginosa* lacks the ability to distinguish between phages that  
3 enter lytic or lysogenic cycles.

4         Given these opposing fitness effects of CRISPR-Cas immune systems during  
5 horizontal<sup>2,3</sup>, and vertical transmission of DMS3 (Fig. 3), it is unclear what the net fitness  
6 effects of CRISPR-Cas systems are during temperate phage infections. To explore this, we  
7 competed WT and  $\Delta cas7$  strains in the presence of either DMS3*vir*, DMS3, DMS3-*acrIF1* or  
8 DMS3-*acrIF4* phages and determined their relative fitness at day 1, 3 and 7. Strikingly, while  
9 WT bacteria were fitter than  $\Delta cas7$  in the presence of virulent phage (Fig. 4a, one-tailed  
10 Wilcoxon test, relative fitness  $>1$ ;  $p=0.016$ ), they were considerably less fit during temperate  
11 phage infection (Fig. 4a, relative fitness  $<1$ ;  $p=0.018$ ), unless the temperate phage carried *acr*  
12 genes (Fig. 4a, relative fitness  $\neq 1$ ;  $p=0.16$ ). Hence, in this context *acr* genes not only provide  
13 a benefit to the phage during both horizontal<sup>3,17,18</sup> and vertical transmission (Fig. 4b, one-tailed  
14 t-test: relative fitness  $\neq 1$ , *acrIF1*;  $t_5=39.30$ ,  $p<0.0001$ ; *acrIF4*;  $t_5=11.61$ ,  $p<0.0001$ ), but also to  
15 the host by preventing autoimmunity.

16

### 17 **Bacteria evolve to lose CRISPR-Cas**

18 We next monitored whether WT lysogens evolved to alleviate these autoimmunity costs  
19 through mutation of their immune system or the prophage. Lysogens in WT and adaptation-  
20 deficient  $\Delta cas1$  backgrounds, which had reduced growth during early infection, were selected  
21 from the late infection stage (7 dpi). Growth curves revealed that the negative fitness  
22 consequences of CRISPR-Cas immune systems had disappeared in these “late lysogens”,  
23 and they now had growth rates comparable to ancestral hosts lacking the prophage (Fig. 4c,d,  
24 compare to Fig. 3a,b). A competition experiment confirmed this finding, showing that late  
25 lysogens in a WT background were fitter than a surface mutant (Fig. 4e, one-tailed t-test,  
26 relative fitness  $>1$ ;  $t_5=5.985$ ,  $p<0.001$ ), and the presence of *acr* genes in the prophage no  
27 longer increased the fitness of the host (Fig. 4e, one-tailed t-test: *acrIF1*;  $t_5=-5.5085$ ,  $p=1.00$ ;  
28 *acrIF4*;  $t_5=-2.0395$ ,  $p=0.95$ ) (compare to Fig. 3e).

1           To understand the mechanistic basis for this alleviation in fitness costs, we performed  
2 PCR analyses of the CRISPR loci of 6 independent lysogens in WT,  $\Delta cas1$  and  $\Delta cas7$   
3 backgrounds, isolated from early or late time points after infection. Both CRISPR loci (1 and  
4 2) amplified as expected in early lysogens (Extended Data Fig. 4a), however, amplification  
5 failed in many late lysogens in WT and  $\Delta cas1$  backgrounds (Extended Data Fig. 4a, negative  
6 PCR indicated by red frame), suggesting that the CRISPR-Cas locus was lost in these clones.  
7 Whole genome sequencing of late lysogens revealed large genomic deletions associated with  
8 prophage integration (between ~ 50 and 230 kb) that encompassed the entire CRISPR-Cas  
9 locus - but contained no essential gene<sup>19</sup> - in WT and  $\Delta cas1$  backgrounds, while the genome  
10 remained intact in  $\Delta cas7$  late lysogens (Extended Data Fig. 4c-e and Extended Data Table 1).  
11 This loss of the CRISPR-Cas locus was clearly driven by the immunopathological effects of  
12 CRISPR 2 spacer 1, as the locus was maintained in lysogens lacking CRISPR 2 ( $\Delta CRISPR2$ )  
13 but lost when expression of spacer 1 was restored ( $\Delta CRISPR2$ -sp1) (Extended Data Fig. 2b).  
14 The loss of CRISPR-Cas was also avoided when WT bacteria were lysogenized by DMS3  
15 carrying *acr* genes (Extended Data Fig. 4a).

16

### 17 **Generality of the empirical data**

18 Collectively, these data show that temperate phage infection can drive rapid loss of CRISPR-  
19 Cas immune systems from bacterial genomes due to immunopathological effects that manifest  
20 during vertical transmission. To generalize our findings beyond phage DMS3 (belonging to  
21 *Caudovirales*), we introduced a priming spacer with one mismatch against the Pf5 prophage  
22 (*Inoviridae*) that is naturally present in the genome of WT PA14<sup>20</sup>. Expression of a Pf5-priming  
23 spacer caused reduced growth of the WT strain and strong selection for bacteria carrying a  
24 deletion in their CRISPR-Cas immune system (Extended Data Fig. 5). These observations  
25 therefore suggest that immunopathological effects generally drive selection for CRISPR loss,  
26 whenever hosts carry spacers primed against their prophage. Indeed, when we formalized  
27 these ideas in a theoretical framework, we recovered very similar population and evolutionary



1 dynamics as those observed in our experiments (Extended Data Fig. 6; See Supplemental  
2 Information for a detailed description of the model).

3         Crucially, priming is thought to be frequent in nature due to the relaxed sequence  
4 identity requirements for triggering this pathway, with up to 13 mismatches between a pre-  
5 existing spacer and the target being tolerated<sup>7</sup>. Indeed, analysis of the spacers from >170k  
6 bacterial genomes and a dataset of ~20k prophages<sup>21</sup> revealed that pre-existing spacers with  
7 perfect or imperfect (1-5 mismatches) targets to temperate phages are common within genera  
8 (Extended Data Fig. 7; see also Supplemental Information for further information). On  
9 average, 49% of all prophages were targeted by priming spacers carried by bacteria within  
10 the same genera as the lysogen (Extended Data Fig. 7c). If mismatched spacers generally  
11 cause residual DNA cleavage activity by the CRISPR immune system, they would be expected  
12 to cause similar immunopathological effects as those observed for the *P. aeruginosa*-DMS3  
13 interaction. Indeed, when all complete *P. aeruginosa* genomes were assessed, we observed  
14 a significant enrichment for an increase in *acr* frequency when self-targeting spacers matched  
15 prophages (Extended Data Fig. 8), which is consistent with the idea that these spacers cause  
16 immunopathological effects. Together, these bioinformatic analyses suggest that maladaptive  
17 effects of CRISPR-Cas against temperate phages are likely common in nature.

18         In natural ecosystems, bacteria are frequently exposed to both temperate and virulent  
19 phages, and the latter may superinfect the lysogens. To further generalize our findings, we  
20 explored whether these superinfections would likely change the observed population and  
21 evolutionary dynamics. We found that mixed infection of WT PA14 with temperate phage  
22 DMS3 and virulent phage LMA2 (which can superinfect DMS3 lysogens) resulted in similar  
23 rates of lysogenization (Extended Data Fig. 9d,e) and high fitness costs of CRISPR-Cas  
24 (Extended Data Fig. 9g), that drive evolutionary loss of the immune system (Extended Data  
25 Fig. 9f). Our theoretical model recovered similar dynamics, independent of whether CRISPR-  
26 based resistance evolves against only one (as in our experiment) or against both phages  
27 (Extended Data Fig. 9h-o).

28

## 1 Discussion

2 The observation that approximately 60% of all bacterial genotypes lack CRISPR-Cas systems  
3 and that closely related strains differ in whether they encode *cas* genes suggests that these  
4 systems are frequently gained and lost from bacterial genomes<sup>22</sup>. While phage infection is  
5 typically assumed to be an important selective force for the maintenance of CRISPR-Cas  
6 immune systems, this work reveals their rapid loss when exposed to a temperate phage, as a  
7 result of immunopathological effects when the CRISPR immune system is “primed” against  
8 this phage. Certain CRISPR-Cas immune systems may mitigate some of these autoimmunity  
9 costs by limiting the spacer acquisition and cleavage of transcriptionally silent elements<sup>15,23</sup>.  
10 However, CRISPR-based autoimmunity is frequently reported<sup>24–27</sup>, and the high frequencies  
11 at which primed self-targeting interactions occur suggests this is likely a major driver of the  
12 evolutionary loss of CRISPR systems in nature.

13

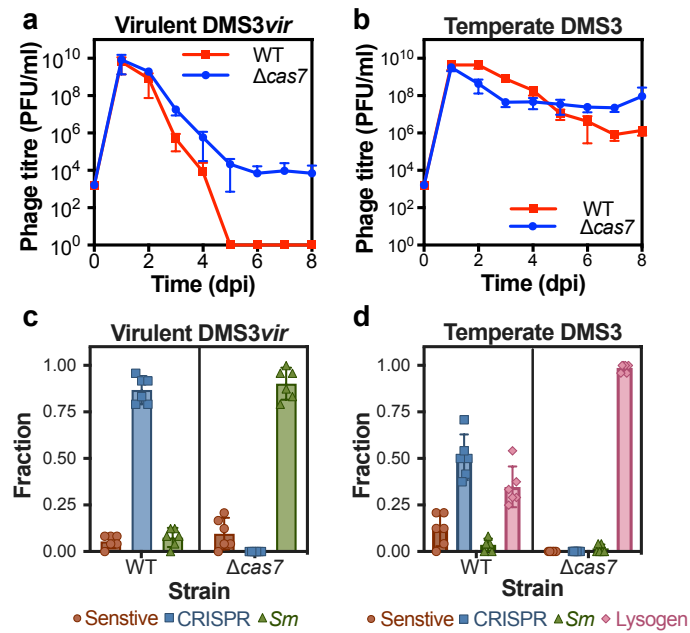
## 14 References

- 15 1. Stewart, F. M. & Levin, B. R. The population biology of bacterial viruses: Why be temperate.  
16 *Theor. Popul. Biol.* **26**, 93–117 (1984).
- 17 2. Westra, E. R. *et al.* Parasite Exposure Drives Selective Evolution of Constitutive versus Inducible  
18 Defense. *Curr. Biol.* **25**, 1043–1049 (2015).
- 19 3. van Houte, S. *et al.* The diversity-generating benefits of a prokaryotic adaptive immune system.  
20 *Nature* **532**, 385–388 (2016).
- 21 4. Barrangou, R. *et al.* CRISPR Provides Acquired Resistance Against Viruses in Prokaryotes.  
22 *Science* **315**, 1709–1712 (2007).
- 23 5. Garneau, J. E. *et al.* The CRISPR/Cas bacterial immune system cleaves bacteriophage and  
24 plasmid DNA. *Nature* **468**, 67–71 (2010).
- 25 6. Datsenko, K. A. *et al.* Molecular memory of prior infections activates the CRISPR/Cas adaptive  
26 bacterial immunity system. *Nat. Commun.* **3**, 1–7 (2012).
- 27 7. Fineran, P. C. *et al.* Degenerate target sites mediate rapid primed CRISPR adaptation. *Proc. Natl.*  
28 *Acad. Sci.* **111**, E1629–E1638 (2014).

- 1 8. Howard-Varona, C., Hargreaves, K. R., Abedon, S. T. & Sullivan, M. B. Lysogeny in nature:  
2 mechanisms, impact and ecology of temperate phages. *ISME J.* **11**, 1511–1520 (2017).
- 3 9. Heussler, G. E. *et al.* Clustered Regularly Interspaced Short Palindromic Repeat-Dependent,  
4 Biofilm-Specific Death of *Pseudomonas aeruginosa* Mediated by Increased Expression of Phage-  
5 Related Genes. *mBio* **6**, e00129-15 (2015).
- 6 10. Zegans, M. E. *et al.* Interaction between Bacteriophage DMS3 and Host CRISPR Region Inhibits  
7 Group Behaviors of *Pseudomonas aeruginosa*. *J. Bacteriol.* **191**, 210–219 (2009).
- 8 11. Berngruber, T. W., Froissart, R., Choisy, M. & Gandon, S. Evolution of Virulence in Emerging  
9 Epidemics. *PLoS Pathog.* **9**, e1003209 (2013).
- 10 12. Trasanidou, D. *et al.* Keeping crisper in check: diverse mechanisms of phage-encoded anti-crisprs.  
11 *FEMS Microbiol. Lett.* **366**, fnz098 (2019).
- 12 13. Bondy-Denomy, J. *et al.* Multiple mechanisms for CRISPR–Cas inhibition by anti-CRISPR  
13 proteins. *Nature* **526**, 136–139 (2015).
- 14 14. Little, J. W. & Michalowski, C. B. Stability and Instability in the Lysogenic State of Phage Lambda.  
15 *J. Bacteriol.* **192**, 6064–6076 (2010).
- 16 15. Goldberg, G. W., Jiang, W., Bikard, D. & Marraffini, L. a. Conditional tolerance of temperate  
17 phages via transcription-dependent CRISPR-Cas targeting. *Nature* **514**, 633–637 (2014).
- 18 16. Samai, P. *et al.* Co-transcriptional DNA and RNA cleavage during type III CRISPR-Cas immunity.  
19 *Cell* **161**, 1164–1174 (2015).
- 20 17. Landsberger, M. *et al.* Anti-CRISPR Phages Cooperate to Overcome CRISPR-Cas Immunity.  
21 *Cell* **174**, 908-916.e12 (2018).
- 22 18. Borges, A. L. *et al.* Bacteriophage Cooperation Suppresses CRISPR-Cas3 and Cas9 Immunity.  
23 *Cell* **174**, 917-925.e10 (2018).
- 24 19. Poulsen, B. E. *et al.* Defining the core essential genome of *Pseudomonas aeruginosa*. *Proc. Natl.*  
25 *Acad. Sci.* 201900570 (2019). doi:10.1073/pnas.1900570116
- 26 20. Mooij, M. J. *et al.* Characterization of the integrated filamentous phage Pf5 and its involvement in  
27 small-colony formation. *Microbiology* **153**, 1790–1798 (2007).
- 28 21. Zhou, Y., Liang, Y., Lynch, K. H., Dennis, J. J. & Wishart, D. S. PHAST: a fast phage search tool.  
29 *Nucleic Acids Res.* **39**, W347-352 (2011).

- 1 22. Makarova, K. S. *et al.* An updated evolutionary classification of CRISPR–Cas systems. *Nat. Rev.*  
2 *Microbiol.* **13**, 722–736 (2015).
- 3 23. Levy, A. *et al.* CRISPR adaptation biases explain preference for acquisition of foreign DNA.  
4 *Nature* **520**, 505–510 (2015).
- 5 24. Stern, A., Keren, L., Wurtzel, O., Amitai, G. & Sorek, R. Self-targeting by CRISPR: Gene  
6 regulation or autoimmunity? *Trends Genet.* **26**, 335–340 (2010).
- 7 25. Vercoe, R. B. *et al.* Cytotoxic Chromosomal Targeting by CRISPR/Cas Systems Can Reshape  
8 Bacterial Genomes and Expel or Remodel Pathogenicity Islands. *PLoS Genet.* **9**, e1003454  
9 (2013).
- 10 26. Jiang, W. *et al.* Dealing with the Evolutionary Downside of CRISPR Immunity: Bacteria and  
11 Beneficial Plasmids. *PLoS Genet.* **9**, e1003844 (2013).
- 12 27. Goldberg, G. W. *et al.* Incomplete prophage tolerance by type III-A CRISPR-Cas systems  
13 reduces the fitness of lysogenic hosts. *Nat. Commun.* **9**, 61 (2018).
- 14  
15

# 1 Main Figures



2

## 3 Figure 1 | Phage persistence and host resistance evolution upon virulent or temperate phage

4 infections. (a) Phage densities over time following infection of WT PA14 or the  $\Delta cas7$  mutant with

5 DMS3vir or (b) DMS3. The limit of phage detection is 200 PFU/ml. (c) Fraction of bacteria that had

6 evolved resistance at 3 dpi following infection with phage DMS3vir or (d) DMS3, either through CRISPR-

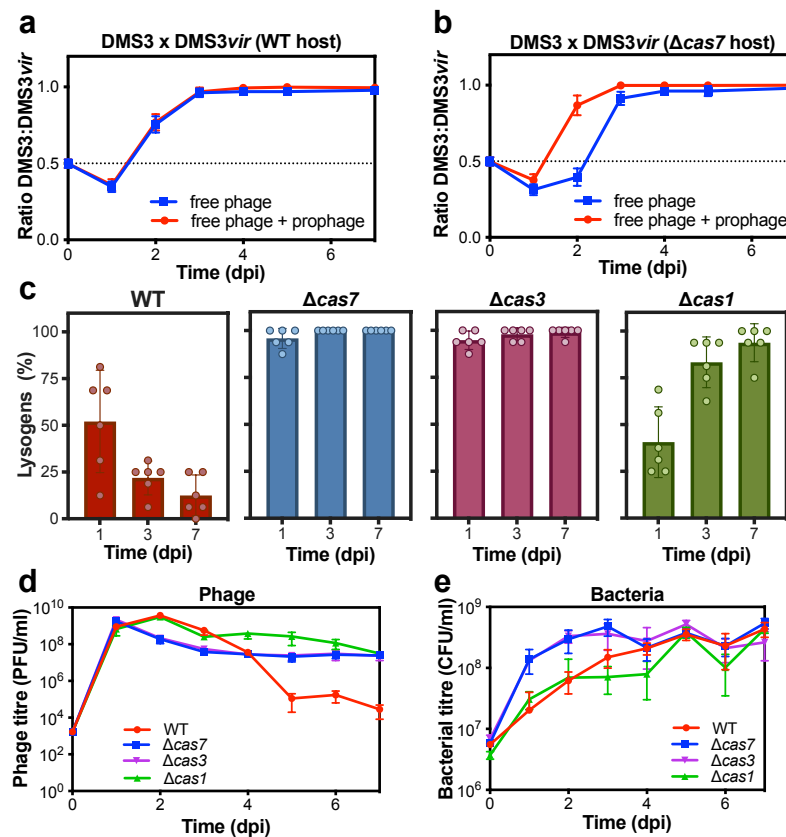
7 Cas (CRISPR), surface modification (sm) or lysogeny (Lysogen). Fractions are based on 24 random

8 clones per replicate experiment. In all panels, data shown are the mean of 6 biologically independent

9 replicates per treatment. Error bars represent 95 % confidence intervals (c.i.).

10

1



2

3 **Figure 2 | The impact of CRISPR adaptation and interference on lysogeny and phage**

4 **persistence. (a)** Relative frequency of DMS3 over time following infection of WT PA14 or **(b)** the  $\Delta cas7$

5 mutant host with an equal mix of DMS3 and DMS3vir. Relative frequencies are shown both for the free

6 and total (i.e. including lysogens) phage population. **(c)** Percentage of DMS3 lysogens in the host

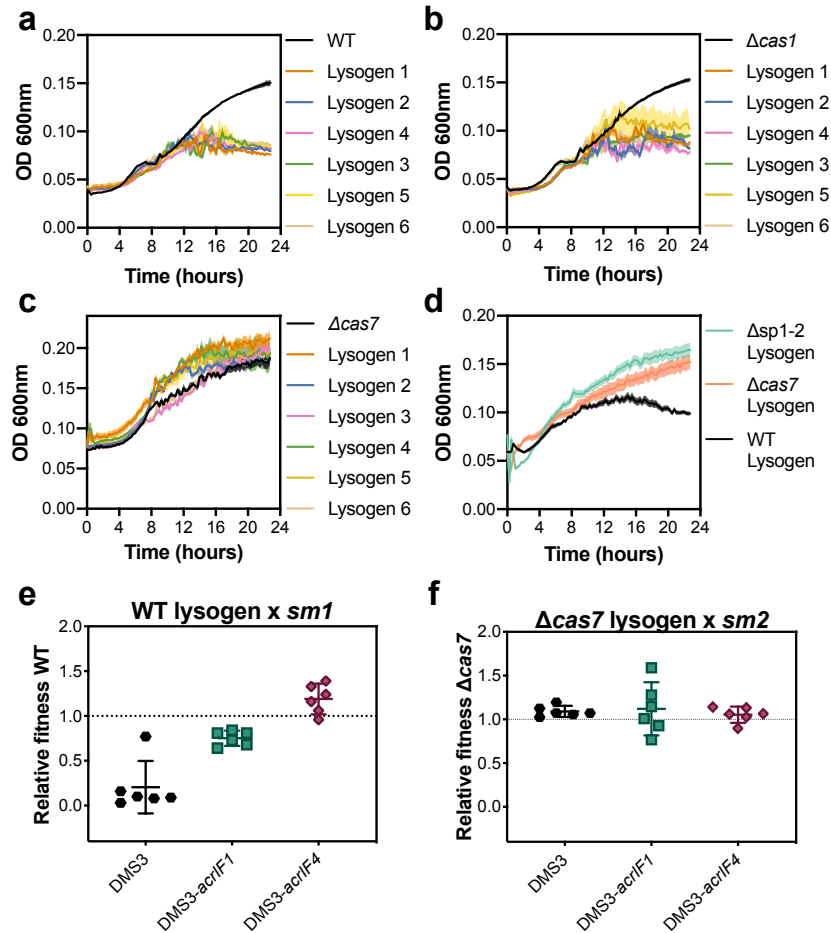
7 population at 1, 3, or 7 dpi of either the WT PA14 strain, the isogenic CRISPR-interference deficient

8 mutants  $\Delta cas7$  and  $\Delta cas3$ , or the isogenic CRISPR-adaptation deficient mutant  $\Delta cas1$ , based on 24

9 random clones per replicate experiment per time point. **(d)** DMS3 phage and **(e)** bacterial densities

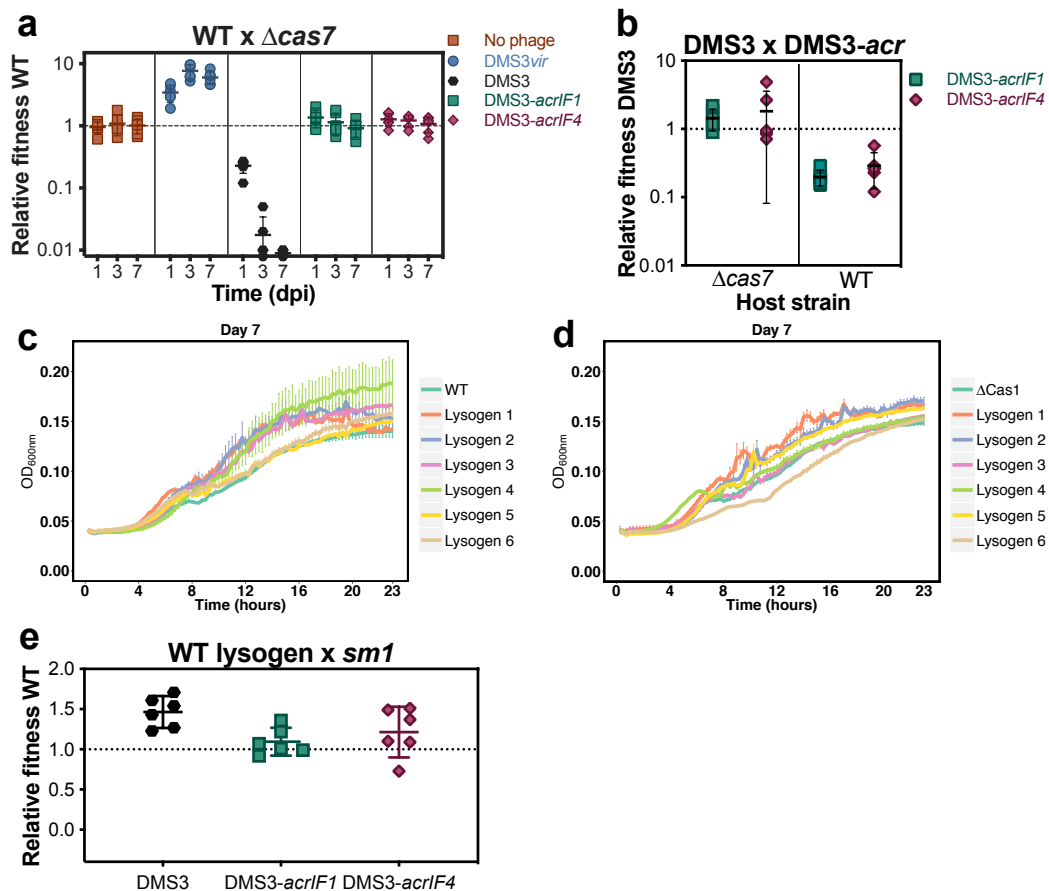
10 during this co-culture experiment. In all panels, data shown are the mean of 6 biologically independent

11 replicates per treatment. Error bars represent 95 % c.i.



1  
2  
3  
4  
5  
6  
7  
8  
9  
10  
11  
12  
13  
14

**Figure 3 | Fitness of lysogens with an active CRISPR-Cas system is reduced unless they encode *acr* genes.** (a) 24-hour growth curves of uninfected control cultures, or 6 independent DMS3 lysogens in WT PA14, (b)  $\Delta cas1$  (CRISPR-adaptation deficient), and (c)  $\Delta cas7$  (CRISPR-interference deficient) genetic backgrounds. Lysogens were isolated from day 1 of the co-culture experiment shown in Fig. 2. Curves are the mean of 6 (a,b) or 4 (c) replicates and shaded areas represent standard error of the mean. (d) 24-hour mean growth curves of 6 lysogens in WT,  $\Delta cas7$  and  $\Delta sp1-2$  (carrying a deletion of CRISPR2 spacers 1 and 2) backgrounds isolated from 6 biological replicates. Each growth curve was performed in 5 technical replicates. Shaded areas represent standard error of the mean. (e) Fitness relative to a surface mutant (*sm*) of WT PA14 lysogens isolated 1 day post infection with DMS3 or (f) PA14  $\Delta cas7$  lysogens isolated 1 day post infection with DMS3. Relative fitness was determined after 1 day of competition. Each point represents the average relative fitness of one independent lysogen clone measured across 6 biologically independent experiments and error bars indicate 95% c.i.



1  
2  
3  
4  
5  
6  
7  
8  
9  
10  
11  
12  
13  
14

**Figure 4 | Lysogens evolve to mitigate fitness costs.** (a) Relative fitness of WT during competition with  $\Delta cas7$  hosts following infection with  $10^4$  PFU of either DMS3, the lytic mutant DMS3vir, or the anti-CRISPR-encoding mutants DMS3-acrIF1 and DMS3-acrIF4. (b) Relative fitness of DMS3 (free phages + lysogens) following 3 days of competition with DMS3-acrIF1 or DMS3-acrIF4 on either WT PA14 or  $\Delta cas7$  mutant. (c) 24-hour growth curves of uninfected control cultures, or 6 biologically independent DMS3 lysogens in the WT PA14 or (d)  $\Delta cas1$  genetic backgrounds, which were isolated from day 7 of the co-culture experiment shown in Fig. 2. Curves are the mean of 6 replicates and error bars represent standard error of the mean. (e) Relative fitness of a DMS3 lysogen in a WT PA14 genetic background, isolated from day 5 of a co-culture experiment, during competition with a surface mutant. Relative fitness was calculated after 1 day of competition. All panels show the mean of 6 biologically independent replicates per treatment. Error bars represent 95 % c.i. (panels a,b and e) or standard error of the mean (panels c and d).



## 1 **Methods**

### 2 ***Bacterial strains and viruses***

3 *P. aeruginosa* UCBPP-PA14 (referred to as WT) and *P. aeruginosa* UCBPP-PA14 *csy3::lacZ*  
4 (referred to as  $\Delta cas7$ ) were used in all experiments (described previously<sup>28</sup>). The surface  
5 mutant *Tn::pilA* lacking a pilus (referred to as *sm2*) has been described previously<sup>29</sup> and was  
6 used in competition experiments with bacteriophage insensitive mutant (BIM) with 2 additional  
7 acquired spacers over those present in the WT strain (as described previously<sup>2</sup>).  
8 Lysogens in WT or *cas* mutant backgrounds used in growth curves, fitness and induction  
9 experiments were generated in this study and the presence of a prophage was confirmed by  
10 PCR. PA14 strains  $\Delta cas3$ ,  $\Delta cas1$ ,  $\Delta CRISPR2$  and CRISPR2  $\Delta spacer1-2$ , respectively  
11 identified as SMC4268, SMC4277 and SMC3895 and SMC4707, were described  
12 elsewhere<sup>10,28</sup>.

13 Phage amplifications were carried out on *P. aeruginosa* UCBPP-PA14 *csy3::lacZ*. DMS3 and  
14 the obligately lytic variant DMS3*vir* have been described previously<sup>30</sup>. DMS3-*acrIF1* and  
15 DMS3-*acrIF4* phages were generated in this study following the method for hybrid phage  
16 construction detailed in an earlier study<sup>17</sup>. DMS3*vir-acrIF1* was used in downstream analyses  
17 and has been described elsewhere<sup>3</sup>. A virulent phage capable of infecting DMS3 lysogens  
18 (LMA2, described previously<sup>31</sup>) was used in co-culture experiments.

19 All bacterial strains were grown at 37°C in LB broth or M9 medium (22 mM Na<sub>2</sub>HPO<sub>4</sub>; 22 mM  
20 KH<sub>2</sub>PO<sub>4</sub>; 8.6 mM NaCl; 20 mM NH<sub>4</sub>Cl; 1 mM MgSO<sub>4</sub>; 0.1 mM CaCl<sub>2</sub>) supplemented with 0.2%  
21 glucose. When appropriate, medium was further supplemented with gentamycin (50 mg/ml)  
22 and arabinose (1% w/v).

23

### 24 ***Evolution experiments***

25 To monitor the evolution of bacterial resistance in response to phage infection and the  
26 associated bacterial and phage population dynamics, microcosms with 6 ml of M9 medium  
27 supplemented with 0.2% glucose were inoculated with approximately 10<sup>6</sup> colony forming units  
28 (CFU) bacteria from fresh overnight cultures of the corresponding bacterial strains. These

1 cultures were infected with  $10^4$  plaque forming units (PFU) of DMS3*vir*, DMS3, DMS3-*acrIF*  
2 or LMA2 phages, followed by incubation at 37°C and shaking at 180 revolutions per minute  
3 (rpm). Cultures were transferred 1:100 into fresh medium every 24 hours for 5-8 days. All  
4 experiments were performed in 6 independent replicates.

#### 5 **Determination of resistance phenotypes**

6 Resistance phenotypes were determined at day 3 or day 7 by streaking individual colonies  
7 (24 randomly picked per replicate) through DMS3*vir* and phage DMS3*vir-acrIF1*. Surface  
8 modification was confirmed by colony morphology, broad-range resistance to DMS3*vir* and  
9 DMS3*vir-acrIF1*, and a lack of newly acquired spacers. Lysogens were determined by broad  
10 resistance to both phage and a positive PCR amplification of the c-repressor gene in bacterial  
11 genome, amplified using primers 5'-GCGGAATGAGCGCTAAACC-3' and 5'-  
12 CAAGTGCTTTAGCGAGGAATGC-3'. CRISPR-resistance was confirmed by resistance to  
13 DMS3*vir*, but not to DMS3*vir-acrIF1* and a PCR confirming spacers had been added to one of  
14 the CRISPR arrays. Primers 5'-CTAAGCCTTGACGAAGTCTC-3' and 5'-  
15 CGCCGAAGGCCAGCGCGCCGGTG-3' were used to amplify CRISPR array 1, and primers  
16 5'-GCCGTCCAGAAGTCACCACCCG-3' and 5'-TCAGCAAGTTACGAGACCTCG-3' for  
17 CRISPR array 2. As a positive control for PCR, primers 5'-GCTTGCAGTTCCTCAACGAG-3'  
18 and 5'-CACCAGGAAATTCAGGTAGGG-3' were used to amplify the housekeeping control  
19 gene *fimV* involved in pilus formation.

#### 20 **Bacterial and phage titres**

21 Bacterial densities were determined by plating on LB agar dilutions of samples taken at each  
22 transfer in M9 salts (22 mM Na<sub>2</sub>HPO<sub>4</sub>; 22 mM KH<sub>2</sub>PO<sub>4</sub>; 8.6 mM NaCl; 20 mM NH<sub>4</sub>Cl; 1 mM  
23 MgSO<sub>4</sub>; 0.1 mM CaCl<sub>2</sub>). Phages were extracted at each transfer by chloroform extraction  
24 (sample: chloroform 10:1 v/v), and phage titers were determined by spotting serial dilutions of  
25 isolated phage samples in M9 salts on a lawn of PA14Δ*cas7*.

26

#### 27 **Phage Competition**

#### 28 **Fixed phenotypes**

1 Competition experiments were performed in glass vials in 6 ml of M9 medium. Experiments  
2 were initiated by inoculating a 1:100 dilution of different mixes of overnight cultures of the  
3  $\Delta cas7$  strain and either the surface mutant  $\Delta pilA^{29}$  (*sm2*) or BIM strain (2 spacers targeting  
4 DMS3). A 50:50 mix of phages DMS3*vir* and DMS3 was added ( $10^8$  PFU) and the vials were  
5 incubated at 37°C with shaking for 8 hours. Phages were extracted by chloroform extraction  
6 and spot assays carried out to determine phage titres. To determine phage relative  
7 frequencies, plaque assays were carried out by serially diluting phage extractions and adding  
8 200  $\mu$ l of the selected dilution to 600  $\mu$ l of  $\Delta cas7$  overnight culture and 6 ml molten top agar  
9 (0.5 %), which was then poured over a prewarmed LB agar plate. The plates were incubated  
10 overnight at 37°C and the plaques generated by temperate and virulent phages were  
11 discriminated by differences in opacity, and a subset confirmed by PCR. All experiments were  
12 performed in 6 replicates.

### 13 **Coevolution competitions**

14 Phage competition was also measured in the presence of host evolution. Initially sensitive  
15  $\Delta cas7$  or WT hosts were infected with  $10^4$  PFU of a 50:50 mix of temperate and virulent phages  
16 (DMS3 and DMS3*vir*). The experiment was run as a standard evolution experiment, and  
17 bacterial and phage titres measured every day for 7 days. Resistance phenotypes were  
18 assessed on days 3 and 7, as described above, and plaque assays used to determine the  
19 ratio of temperate to virulent phage at each time point.

### 20 **Competition DMS3 x DMS3-*acrIF***

21 Temperate DMS3 was also competed against a mutant encoding Acr proteins. Initially  
22 sensitive  $\Delta cas7$  or WT hosts were infected with  $10^4$  PFU of a 50:50 mix of DMS3 and DMS3-  
23 *acrIF1* (or DMS3-*acrIF4*). The experiment was run for 3 days and samples of total phage  
24 population (i.e. free phages + prophages, no chloroform extraction) were collected and  
25 immediately frozen every day. Phage titres were measured every day by spot test. To  
26 determine their relative fitness, the relative frequencies of each phage were determined at  
27 T=0 and at T=3 by qPCR, following the method described elsewhere<sup>32</sup>.

28

### 1 ***Expression of priming spacers***

2 The expression of the CRISPR RNA (crRNA) encoding spacer 1 of CRISPR2 was restored in  
3 strain PA14 $\Delta$ CRISPR2 using an arabinose inducible expression vector (pHERD30T-based).  
4 Briefly, oligonucleotides containing the sequences of a non-targeting (NT) spacer (5'-  
5 GTCTTCTTTGAGCTTCCAGAGAACTGAAGAC-3') or of spacer 1 (5'-  
6 ATCAGCCGGACGTTGTAGTAGTCGAGCGCGGT-3') and flanked by two CRISPR2 repeats  
7 were annealed and ligated between NcoI/HindIII restriction sites. The resulting plasmids were  
8 transformed into PA14 $\Delta$ CRISPR2 to generate the strains  $\Delta$ CRISPR2-sp1 and  $\Delta$ CRISPR2-NT,  
9 respectively. Similarly, a spacer targeting the natural Pf5 prophage of PA14 (accession  
10 number AY324828) with 1 mismatch 5'-AGTCCTTCTAGTGAGCGGAACCAAAATCTATT-3'  
11 was expressed in WT PA14 strain.

12

### 13 ***Measuring prophage induction***

14 Single colonies were picked from plated lysogens and grown in LB media overnight at 37°C  
15 with 180 rpm shaking. The overnight culture was diluted 1:100 in fresh M9 media and grown  
16 until optical density (OD<sub>600nm</sub>) reached ~0.1. The cultures were then pelleted by centrifugation  
17 and the pellet washed 5 times in M9 buffer, then resuspended in 10 ml of M9 media. The  
18 cultures were grown at 37°C with shaking and samples taken regularly for phage quantification  
19 by spot assay and OD<sub>600nm</sub> measurements using a Biotek synergy 2 plate reader.

20

### 21 ***24-hour growth curves***

22 Single colonies were isolated and grown in M9 media overnight at 37 °C with 180 rpm shaking.  
23 The following day, this culture was diluted 1:100 and 250  $\mu$ l of this mixture was added to a 96-  
24 well plate and growth curves were measured for 23 hours in a Thermo Scientific Varioskan  
25 flash plate reader with continuous shaking at 180 rpm. Readings of OD<sub>600nm</sub> were taken every  
26 15 minutes and the plate kept at 37°C. All growth curves were performed in 6-12 replicates.

27

### 28 ***Bacterial competition***

1 Competition experiments were performed in 6 ml M9 medium supplemented with 0.2%  
2 glucose. Competition experiments were initiated by inoculating 1:100 from a 1:1 mixture of  
3 overnight cultures (grown in M9 medium + 0.2% glucose) of each strain. If phages were  
4 included, they were added at a concentration of  $10^4$  PFU. Cells were transferred 1:100 daily  
5 into fresh broth. At varying time points, from 1 to 7 days, samples were taken and cells were  
6 serially diluted in M9 salts and plated on LB agar supplemented with  $50 \mu\text{g ml}^{-1}$  X-gal (to allow  
7 discrimination between strains carrying the *lacZ* gene (blue) or those without (white)). All  
8 experiments were performed in 6 replicates. Relative fitness was calculated from changes in  
9 the relative frequencies of blue and white colonies (rel. fitness =  $[(\text{fraction strain A at } t=x) * (1$   
10  $- (\text{fraction stain A at } t=0))] / [(\text{fraction strain A at } t=0) * (1 - (\text{fraction strain A at } t=x))]$ ).

11

### 12 **Whole-genome sequencing and bioinformatic analyses**

13 Lysogen clones in WT,  $\Delta\text{cas7}$  and  $\Delta\text{cas1}$  backgrounds were isolated from the late timepoints  
14 of the evolution experiments. Standard genome sequencing and standard bioinformatic  
15 analyses were provided by MicrobesNG (as described in <http://www.microbesng.uk>). Raw  
16 read sequencing data have been deposited in the European Nucleotide Archive under the  
17 study accession number PRJEB34503. Trimmed reads were mapped to WT PA14 reference  
18 genome (accession number NC\_008463) with Geneious® 9.1.8 software using Bowtie2  
19 mapper<sup>33</sup> to identify the genomic deletion. Reads were also mapped to DMS3 reference  
20 genome (accession number DQ631426) and hybrid reads composed of a 5'-extremity  
21 matching PA14 and a 3'-extremity matching the 5'-end of DMS3 (and vice versa, i.e. reads  
22 composed of a 5'-extremity matching the 3'-end of DMS3 and a 3'-extremity matching PA14)  
23 were extracted. These hybrid reads were then mapped back to PA14 genome to identify  
24 prophage insertion sites.

25

### 26 **Additional references**

27 28. Cady, K. C. & O'Toole, G. A. Non-Identity-Mediated CRISPR-Bacteriophage Interaction Mediated  
28 via the Csy and Cas3 Proteins. *J. Bacteriol.* **193**, 3433–3445 (2011).

- 1 29. Liberati, N. T. *et al.* An ordered, nonredundant library of *Pseudomonas aeruginosa* strain PA14  
2 transposon insertion mutants. *Proc. Natl. Acad. Sci.* **103**, 2833–2838 (2006).
- 3 30. Cady, K. C., Bondy-Denomy, J., Heussler, G. E., Davidson, A. R. & O’Toole, G. A. The  
4 CRISPR/Cas Adaptive Immune System of *Pseudomonas aeruginosa* Mediates Resistance to  
5 Naturally Occurring and Engineered Phages. *J. Bacteriol.* **194**, 5728–5738 (2012).
- 6 31. Ceysens, P.-J. *et al.* Comparative analysis of the widespread and conserved PB1-like viruses  
7 infecting *Pseudomonas aeruginosa*. *Environ. Microbiol.* **11**, 2874–2883 (2009).
- 8 32. Chevallereau, A. *et al.* *Exploitation of the cooperative behaviours of anti-CRISPR phages.*  
9 (bioRxiv Microbiology, 2019). doi:10.1101/574418
- 10 33. Langmead, B. & Salzberg, S. L. Fast gapped-read alignment with Bowtie 2. *Nat. Methods* **9**, 357–  
11 359 (2012).
- 12 34. Biswas, A., Staals, R. H. J., Morales, S. E., Fineran, P. C. & Brown, C. M. CRISPRDetect: A  
13 flexible algorithm to define CRISPR arrays. *BMC Genomics* **17**, 356 (2016).
- 14 35. Couvin, D. *et al.* CRISPRCasFinder, an update of CRISPRFinder, includes a portable version,  
15 enhanced performance and integrates search for Cas proteins. *Nucleic Acids Res.* **46**, W246–  
16 W251 (2018).
- 17 36. Watters, K. E., Fellmann, C., Bai, H. B., Ren, S. M. & Doudna, J. A. Systematic discovery of  
18 natural CRISPR-Cas12a inhibitors. *Science* **362**, 236–239 (2018).
- 19 37. Arndt, D. *et al.* PHASTER: a better, faster version of the PHAST phage search tool. *Nucleic Acids*  
20 *Res.* **44**, W16–W21 (2016).

21  
22

## 1 **Acknowledgements**

2 We thank A.R. Davidson (University of Toronto, Toronto, Canada) for providing the mutant  
3 strains of PA14  $\Delta cas3$ ,  $\Delta cas7$ ,  $\Delta cas1$  and  $\Delta CRISPR2$ , G.A. O'Toole (Dartmouth College, New  
4 Hampshire, USA) for the strain CRISPR2 $\Delta sp1,2$  and J. Bondy-Denomy (University of  
5 California, San Francisco, USA) for the *Tn::pilA* ( $\Delta pilA$ ) PA14 surface mutant. Genome  
6 sequencing was provided by MicrobesNG (<http://www.microbesng.uk>), which is supported by  
7 the BBSRC (grant number BB/L024209/1). This work was funded by a grant from the  
8 European Research Council (<https://erc.europa.eu>) (ERC-STG-2016-714478 - EVOIMMECH)  
9 and NERC Independent Research Fellowship (NE/M018350/1) awarded to E.R.W., A.C. has  
10 received funding from the European Union's Horizon 2020 research and innovation  
11 programme under the Marie Skłodowska-Curie grant agreement No 834052. P.F. was  
12 supported by the Marsden Fund from the Royal Society of New Zealand.

13

## 14 **Author Contributions**

15 Conceptualization of the study was done by C.R, A.C. and E.R.W. Experimental design was  
16 carried out by C.R., A.C., B.N.J.W and E.R.W. Bacterial evolution, competition and growth  
17 experiments were done by C.R. and A.C. with assistance from O.F. and I.M.; Virulent vs  
18 Temperate phage competitions and prophage induction rate experiments were performed by  
19 C.R. All experiments with Acr-phages and CRISPR2 spacer 1 were done by A.C.; B.N.J.W  
20 and A.C. carried out Pf5 experiments. Experiment with superinfecting virulent phage was done  
21 by E.R.W.; C.R., A.C., B.W., T.C., C.B., P.F., and E.R.W. analysed the data. S.G. generated  
22 theoretical mathematical models; T.C. conducted bioinformatic analyses supervised by C.B.  
23 and P.F.; A.C. made whole genome sequencing analyses. C.R. wrote the original draft of the  
24 manuscript; A.C. wrote the revised version of the manuscript with contributions from C.R.,  
25 B.W., T.C., S.G., C.B. and P.F.; E.R.W. supervised the project and provided comments on all  
26 versions of the manuscript.

27

28

1 **Author Information**

2 The authors declare no competing interests. Correspondence and requests for materials  
3 should be addressed to Anne Chevallereau, Clare Rollie or Edze Westra.

4

5 **Data and code availability**

6 Source data associated with main figures and Extended Data Figures 1,2,3,5,7,8 and 9 are  
7 available in the online version of this publication. Sequencing data have been deposited in the  
8 European Nucleotide Archive under the study accession number PRJEB34503. The datasets  
9 analysed for the bioinformatic study are available on github at

10 <https://github.com/davidchyou/Rollie-Chevallereau>

11

12 **Code availability**

13 Mathematical algorithms generated during this study are available in the online supplementary  
14 information file. Scripts generated for the bioinformatics analyses are available on github at

15 <https://github.com/davidchyou/Rollie-Chevallereau>

16



1 **Extended Data Figure Legends**

2 **Extended Data Figure 1 | Infections with a 50:50 mix of temperate:virulent phages.** (a) Bacterial  
3 and (b) phage titres during a co-culture experiment of either WT PA14 (red) or  $\Delta cas7$  mutant (blue) and  
4 a 50:50 mix of DMS3 and DMS3 $vir$ . (c) Resistance phenotypes at day 3 or (d) day 7 of the co-culture  
5 experiment, based on 24 random clones per replicate experiment. Data shown are the mean of 6  
6 biological replicates per treatment. Error bars represent 95 % c.i.

7

8 **Extended Data Figure 2 | Suppression of lysogeny and immunopathological effects are due to**  
9 **spacer 1 of CRISPR array 2.** (a) Phage and (b) bacterial titres during co-culture of phage DMS3 and  
10 *P. aeruginosa* PA14 $\Delta CRISPR2$  expressing either a non-targeting spacer from a plasmid ( $\Delta CRISPR2$ -  
11 NT) or the original CRISPR2 spacer 1 ( $\Delta CRISPR2$ -sp1). (c) The proportion of lysogens and (d) the  
12 frequency of loss of CRISPR-Cas immune systems at 1 and 3 dpi, based on PCR analyses of 24  
13 random clones per replicate experiment. Panels a to d show the mean of 3 biological replicates (error  
14 bars represent 95 % c.i.) (e-g) Growth of 3 independent lysogen clones isolated at 3 dpi as determined  
15 by OD600nm measurements. (e)  $\Delta CRISPR2$ -NT and (f)  $\Delta CRISPR2$ -sp1 lysogen clones carry the  
16 ancestral  $\Delta CRISPR2$  CRISPR-Cas immune system, while (g)  $\Delta CRISPR2$ -sp1 lysogen clones have  
17 evolved to lose CRISPR-Cas.

18

19 **Extended Data Figure 3 | Prophage induction rates are increased in hosts with active CRISPR-**  
20 **Cas.** (a) Percentage lysogens formed upon infection of WT host with DMS3 phages engineered to  
21 produce AcrIF1 or AcrIF4 anti-CRISPR proteins. (b) Optical density and (c) phage titres during growth  
22 of lysogens of DMS3, DMS3-*acrIF1* or DMS3-*acrIF4* in a WT PA14 or  $\Delta cas7$  genetic background. (d)  
23 Relative fitness of DMS3 phage during competition with the virulent mutant DMS3 $vir$  in the presence of  
24 varying fractions of sensitive ( $\Delta cas7$ ) host and resistant hosts with either CRISPR- (BIM) or surface-  
25 based immunity (*sm2*) against these phages. Data show mean fitness at 8 hours post-infection. All  
26 panels show the mean of 6 biological replicates and error bars represent 95 % c.i.

27

28 **Extended Data Figure 4 | Lysogens lose their CRISPR-Cas immune systems.** (a) PCR amplification  
29 of the c-repressor gene of the prophage (*c-rep*, 611 bp), the *fimV* gene (located ~ 1 Mb from the CRISPR  
30 loci, positive control for the PCR, 116 bp) and CRISPR loci 1 (349 bp) and 2 (206 bp) on the host  
31 genome. PCRs were performed on 6 independent DMS3 lysogens in WT,  $\Delta cas1$  and  $\Delta cas7$

1 backgrounds isolated at 1 or 7 dpi as well as on 6 independent lysogens of DMS3, DMS3-*acrIF1* or  
2 DMS3-*acrIF4* (WT background) isolated at 6 or 120 hours post infection. Red frames indicate failure to  
3 amplify a product. PCR amplifications were performed on clones isolated from 3 biological replicate  
4 experiments and produced similar results. For gel source data, see Supplementary Figure 1. **(b)**  
5 Schematic of the CRISPR-Cas locus of PA14 WT which spans a region of around 11 kb. Primers used  
6 to amplify regions of CRISPR arrays 1 or 2 are shown as red arrows. **(c)** Whole genome sequencing of  
7 DMS3 lysogens that lost their CRISPR-Cas system (red frames in panel a) in WT PA14, **(d)**  $\Delta cas1$  or  
8 **(e)**  $\Delta cas7$  backgrounds. Graphs show the read coverage of the region encompassing positions  
9 2,700,000 – 2,970,000 of WT PA14 genome. CRISPR-Cas locus is indicated by a green box on the x-  
10 axis. A genome map depicting coding sequences (yellow arrows) is shown above the graphs. Region  
11 comprised between 2.84-2.88 Mb includes sequences that are repeated elsewhere on PA14 genome,  
12 explaining why reads mapping these positions are still detected in some of the deletion mutants. High  
13 peak at the 3'-end of the CRISPR locus corresponds to the coverage of spacer 20 of CRISPR2 by reads  
14 that derive from DMS3 prophage (5'- and 3' extremities of these reads map to phage genome). Spacer  
15 20 of CRISPR2 has 100% identity to DMS3 but is not immunogenic because there is no consensus  
16 PAM.

17

18 **Extended Data Figure 5 | Expression of Pf5 priming spacer in *P. aeruginosa* PA14.** **(a)** Growth of  
19  $\Delta cas7$  (dashed line) or WT (solid line) clones carrying an expression plasmid encoding a non-targeting  
20 spacer (pNT) or a spacer targeting PA14 natural prophage Pf5 with one mismatch (pPf5-MS) as  
21 determined by OD600nm measurements. Graphs show mean curves from 6 biological replicates and  
22 shaded areas corresponds to 95% c.i. **(b)** Relative fitness of WT pNT or WT pPf5-MS during competition  
23 with  $\Delta cas7$  pNT. Data shown are the mean of 6 biological replicates per treatment. Error bars represent  
24 95 % c.i.

25

26 **Extended Data Figure 6 | Simulations of population and evolutionary dynamics of bacteria-**  
27 **phage interactions, when virulent and temperate phages compete on bacteria with CRISPR-Cas**  
28 **system.** Graphs show densities of **(a)** susceptible hosts, CRISPR-resistant bacteria and lysogens or  
29 **(b)** free viruses over time, as well as **(c)** the frequency of temperate phages in a population composed  
30 of both temperate and virulent types. Note that temperate phages can transmit both horizontally and

1 vertically, whereas virulent phages can transmit only horizontally and cannot superinfect lysogens. **(d)**  
2 Frequency of evolutionary loss of CRISPR-Cas system in the lysogen population over time. The  
3 simulations shown in **(a-d)** reflect the situation where both virulent and temperate phages lack *acr*  
4 genes, whereas **(e-h)** reflect the scenario where the temperate type carries an *acr*.

5

6 **Extended Data Figure 7 | Matches between spacers and temperate phages are widespread. (a)**

7 Total matches between non-redundant spacers (n=1,239,973) from 171,361 RefSeq and Genbank  
8 complete genomes and a non-redundant set of temperate phages (n=19,996)<sup>21</sup>. The counts of perfect  
9 (0) or mis-matched (1-5) targets are shown. As a control, the temperate phages were shuffled ten times  
10 retaining the hexanucleotide content (Control). **(b)** Counts of spacers matching temperate phages from  
11 all genera with over 500 spacer-prophage matches. The total number of spacer-prophage matches is  
12 shown for each genus in brackets (i.e. n=X). Counts of matches are shown (0 or 1-5 mismatches, green  
13 and red). The number of temperate phages analysed is plotted (Prophage, purple) and the matches to  
14 shuffled prophages (Control, blue; not visible as only 0 to 10 counts). **(c)** Percentage of prophages  
15 within each genus that were targeted by self-priming spacers (1-5 mismatches). **(d)** Heatmap of the  
16 distribution of mismatches (0-5). Genera are as in (b) and data is shown as log(Count) for each genus,  
17 as the number of matches varied widely between genera.

18

19 **Extended Data Figure 8 | Self-targeting genomes are enriched for *acr* gene(s).** The number of *P.*

20 *aeruginosa* genomes with complete CRISPR-Cas systems that contain (+) or lack (-) genes encoding  
21 known Acr. For these strains, the total with perfect (0) or mismatched (1-5) self-targeting (ST) spacers  
22 to **(a)** anywhere in the genome or to **(b)** prophages are shown. For complete *P. aeruginosa* genomes  
23 all self-targeting events were analysed for matches to prophages using PHASTER<sup>37</sup>. The greater  
24 number of genomes with *acr* genes (Acr +) and self-targeting (ST +) compared to those without ST is  
25 significant ( $p = 8.14E-05$ , Fisher's exact test, two sided, n=71).

26

27 **Extended Data Figure 9 | Presence of a superinfecting virulent phage does not alter**  
28 **immunopathological effects.** **(a)** Bacterial and **(b-c)** phage titres upon **(b)** individual or **(c)** mixed

29 infection of WT PA14 with phage DMS3 and virulent phage LMA2. **(d-e)** Resistance phenotypes  
30 evolved by bacteria against DMS3 upon **(d)** individual or **(e)** mixed infection. **(f)** Frequency of loss of

1 CRISPR-Cas immune systems upon infection with phage DMS3 or with both phages DMS3 and LMA2,  
2 based on 24 random clones per replicate experiment. (g) Relative fitness of WT PA14 during  
3 competition with PA14  $\Delta cas7$  in the presence or absence of phages DMS3 and LMA2. All panels (a-g)  
4 show means of 6 biological replicates and error bars indicate 95% c.i. (h-o) Simulations of population  
5 and evolutionary dynamics during infection of bacteria carrying CRISPR-Cas systems with a mixed  
6 population of unrelated virulent and temperate phages. Graphs show densities of (h,i) susceptible  
7 hosts, CRISPR-resistant bacteria, lysogens and (j,k) free viruses over time, as well as (l,m) the  
8 frequencies of temperate phages in a population composed of both temperate and virulent types. Note  
9 that temperate phage can transmit both horizontally and vertically, whereas virulent phage can transmit  
10 only horizontally and can superinfect the lysogens (because temperate and virulent phages are  
11 unrelated). (n,o) Frequencies of evolutionary loss of CRISPR-Cas system in the lysogen population  
12 over time. The simulations shown in (h, j, l, n) reflect the scenario where bacteria can evolve CRISPR-  
13 based resistance against both phages, whereas (l, k, m, o) reflects the situation where CRISPR-based  
14 resistance does not evolve against the virulent phage and bacteria instead evolve costly surface-based  
15 resistance (as it is the case in the experiments). See also supplementary information for a detailed  
16 description of the simulations.

17

18 **Extended Data Table 1 | Genomic deletions and prophage insertion sites in DMS3 late lysogen**  
19 **clones.**

20 <sup>a</sup>Sum does not reach 100% as a proportion of hybrid reads that mapped PA14 genome did not allow to  
21 define a potential prophage insertion site.

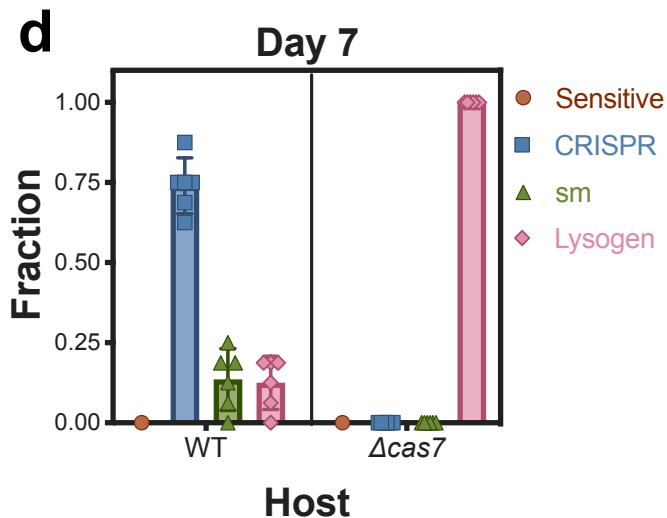
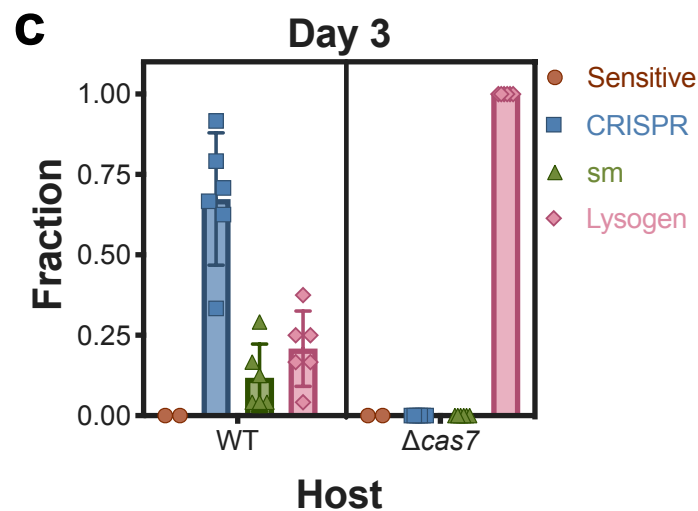
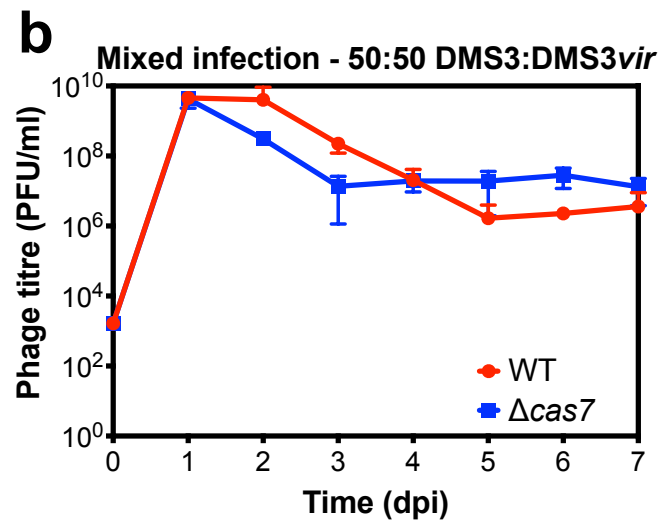
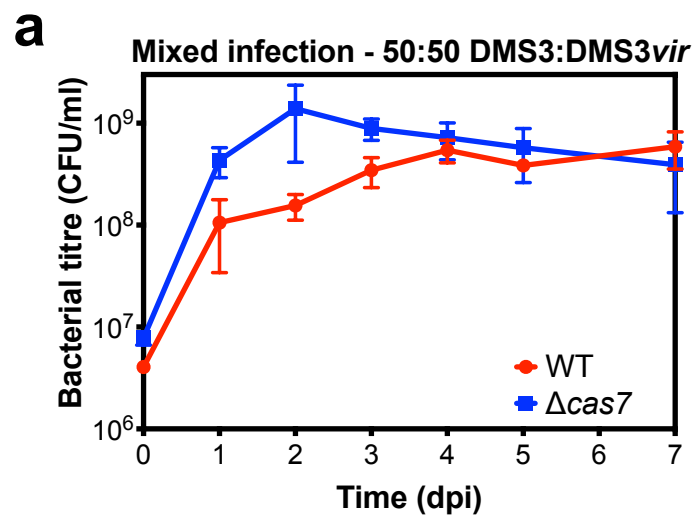
22 <sup>b</sup>Sample contaminated with a Bacteriophage Insensitive Mutant (BIM) clone; sequencing data not  
23 interpretable

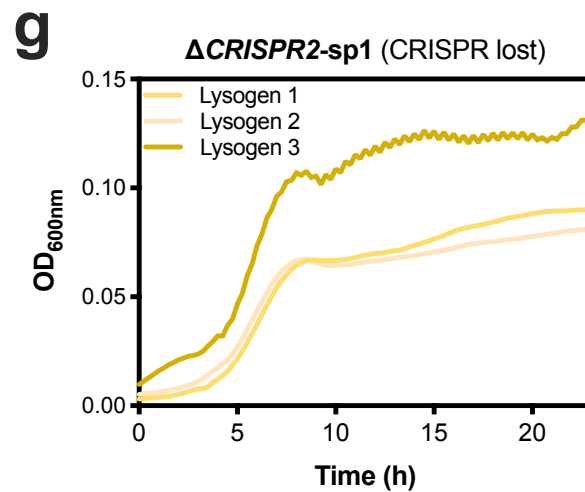
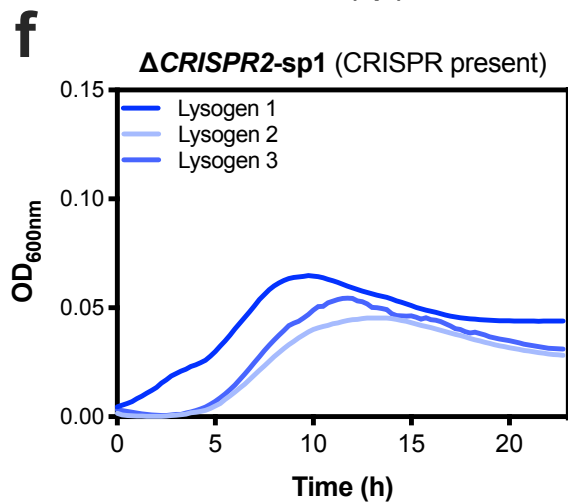
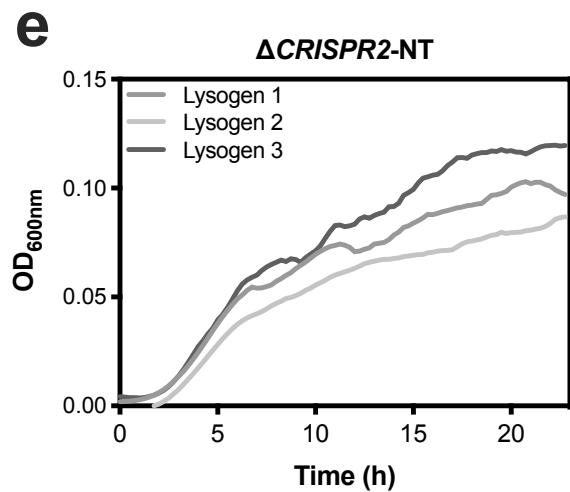
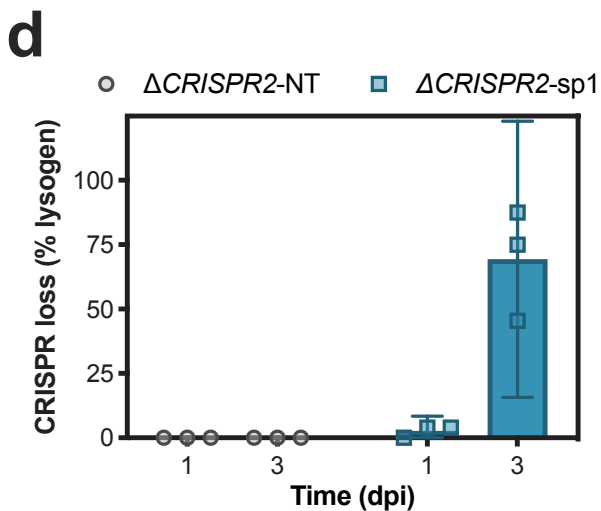
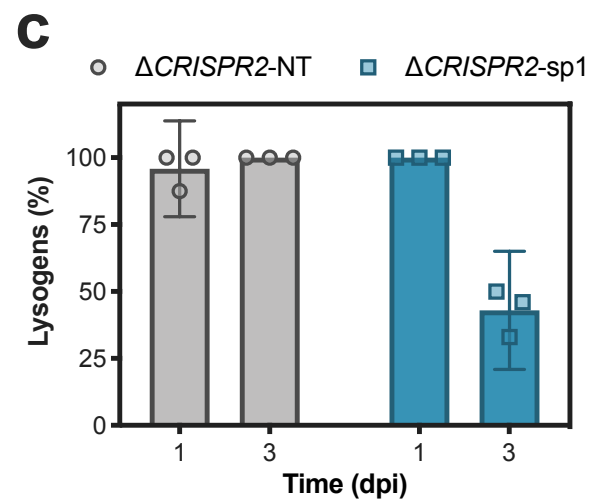
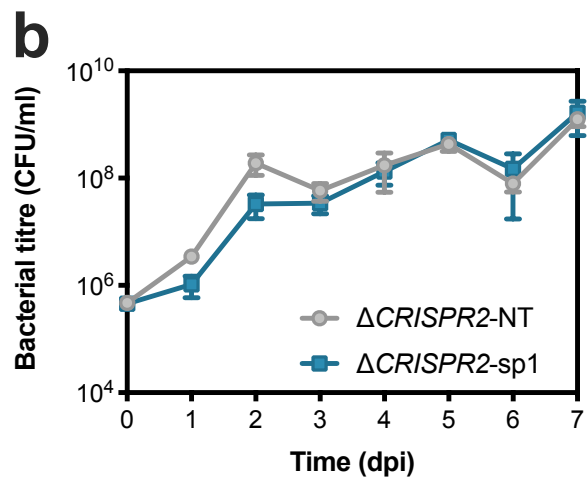
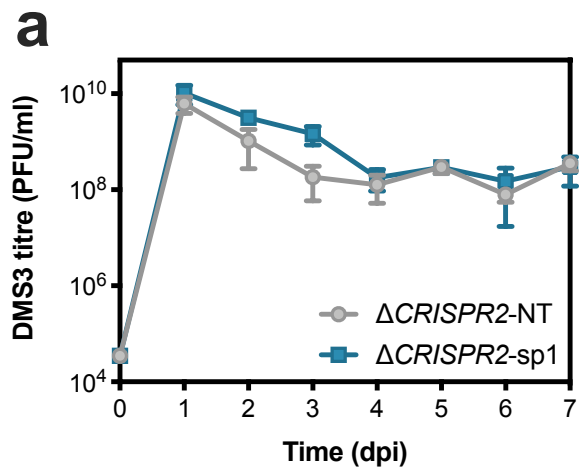
24 <sup>c</sup>Only 2607 bp of DMS3 DNA (including c-repressor gene) are inserted in bacterial genome at position  
25 5,834,730

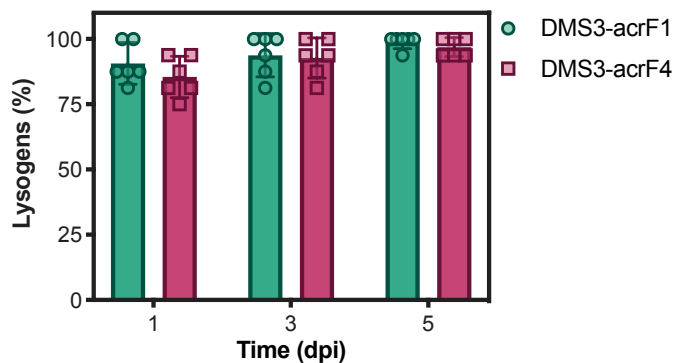
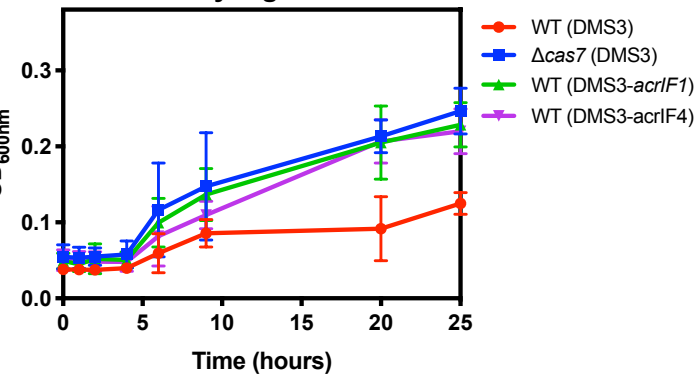
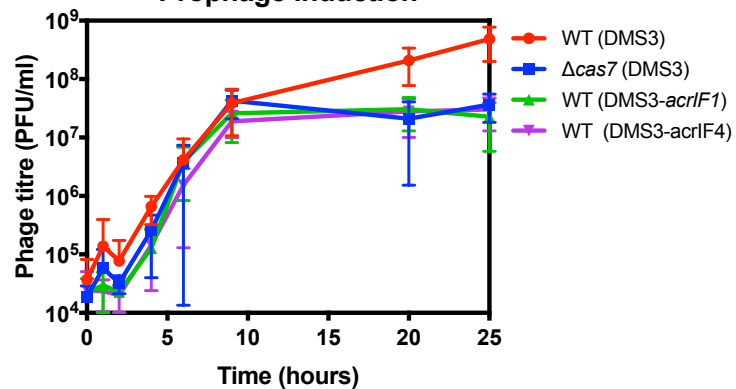
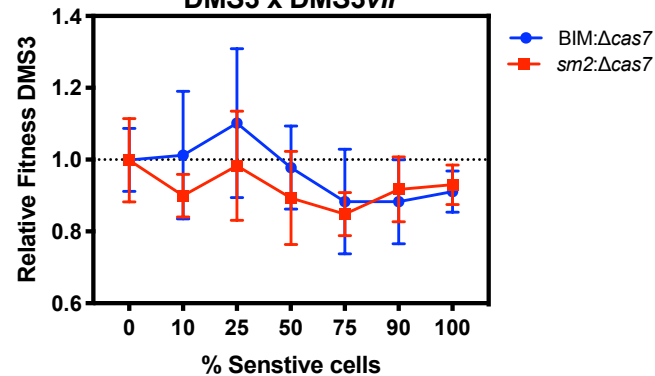
26 <sup>d</sup>Mixed population - reads matching the CRISPR locus are still detectable but coverage is very low

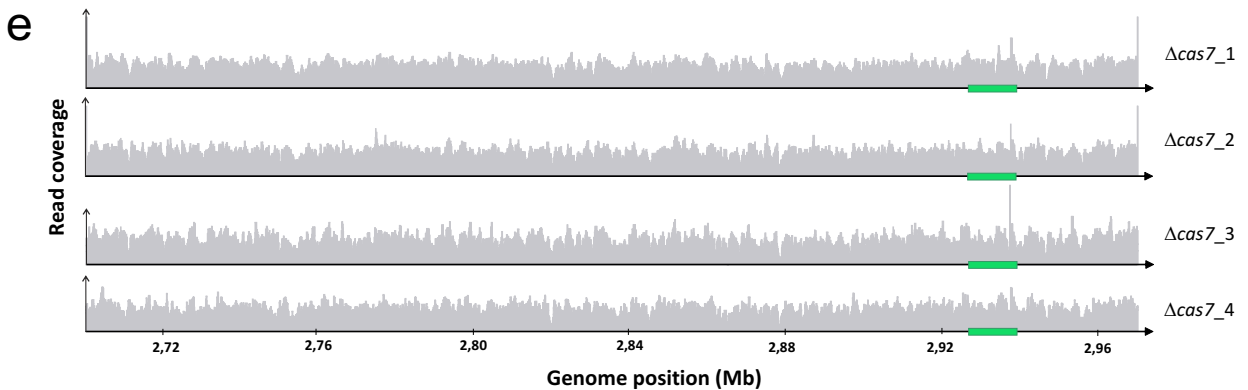
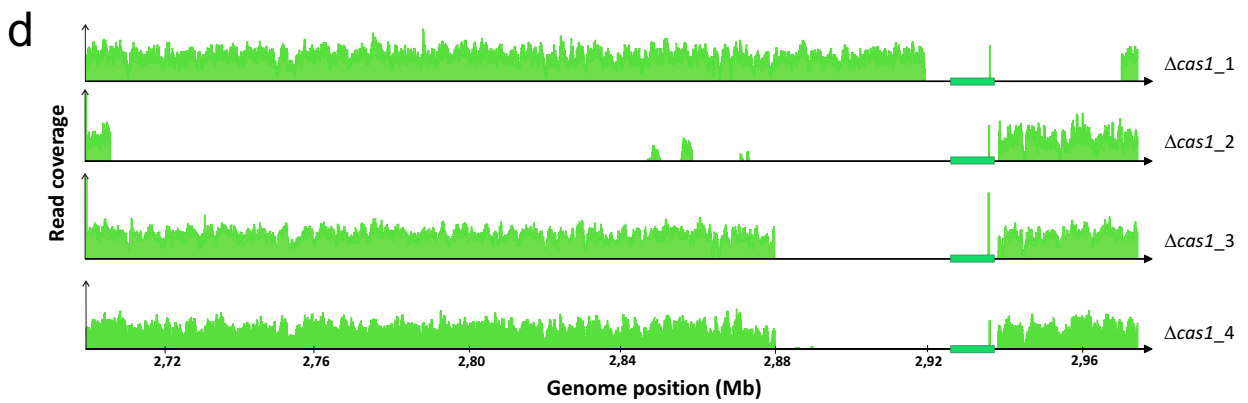
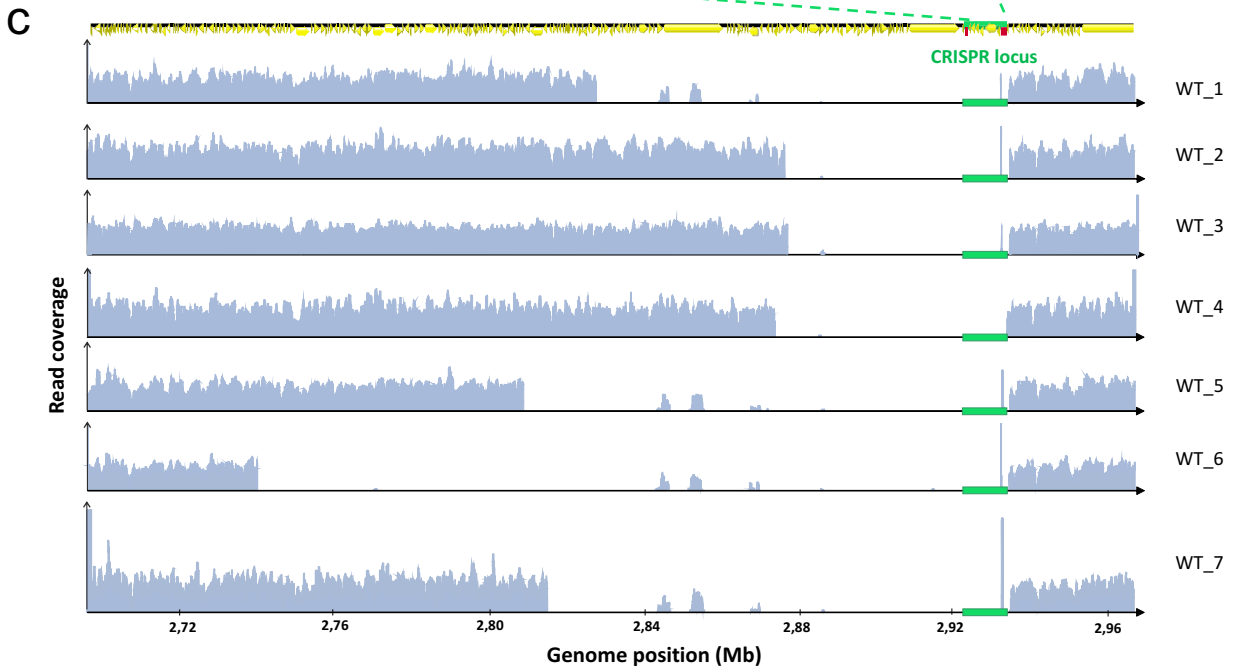
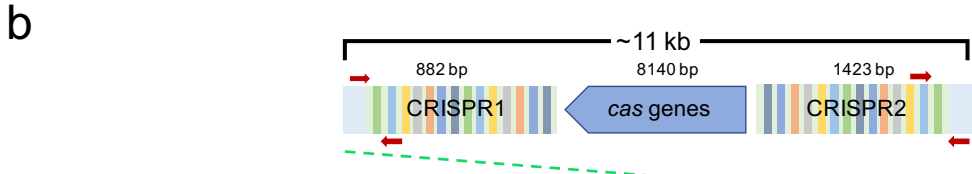
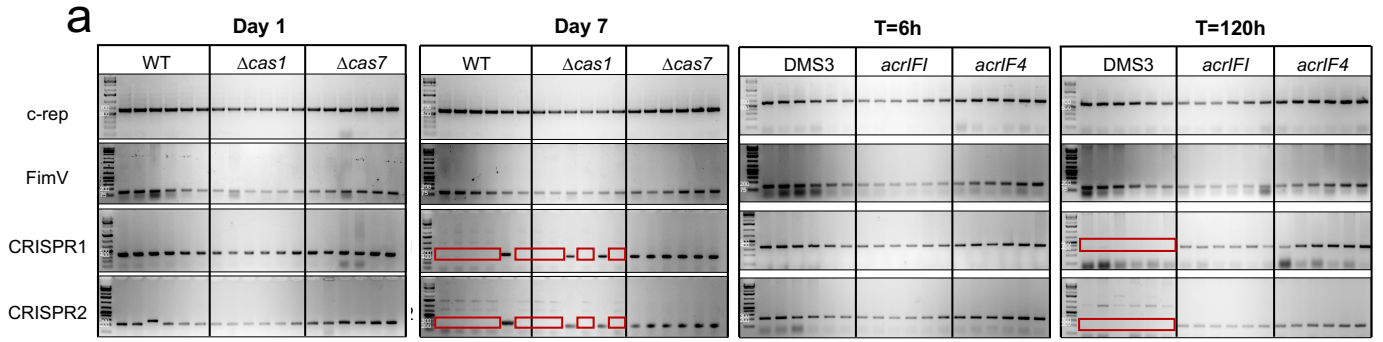
27

28

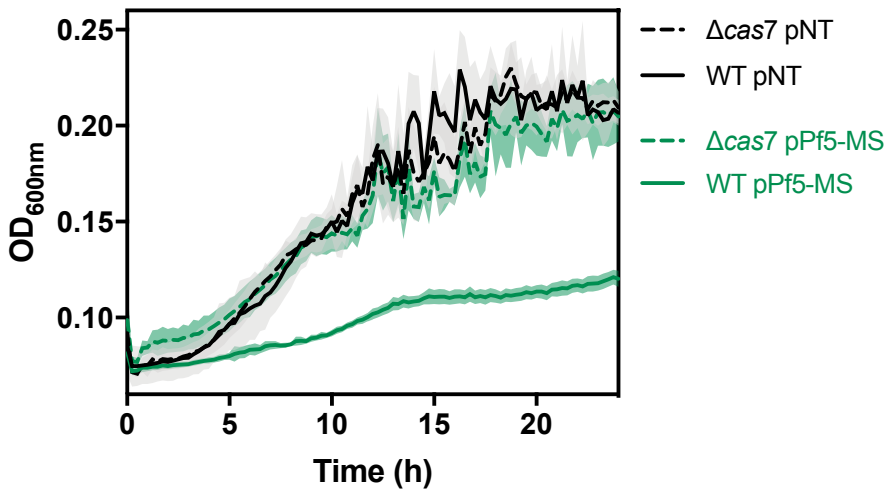
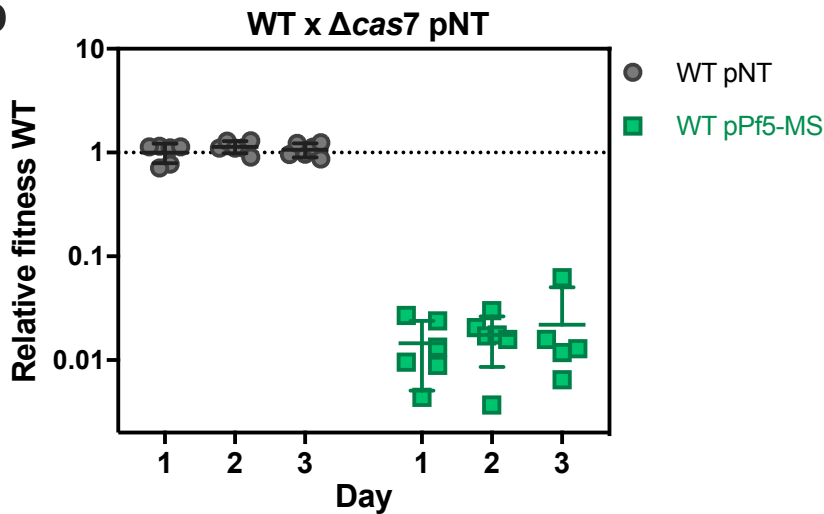


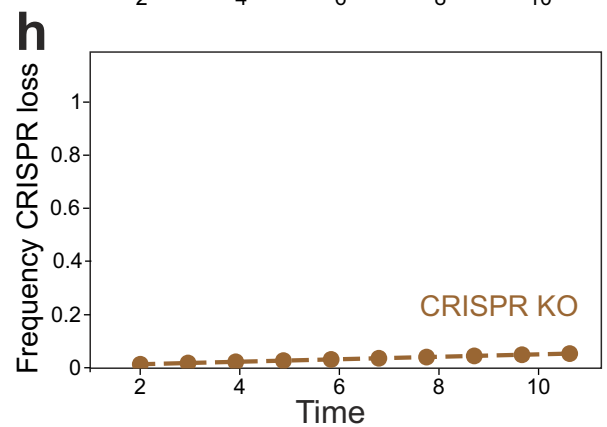
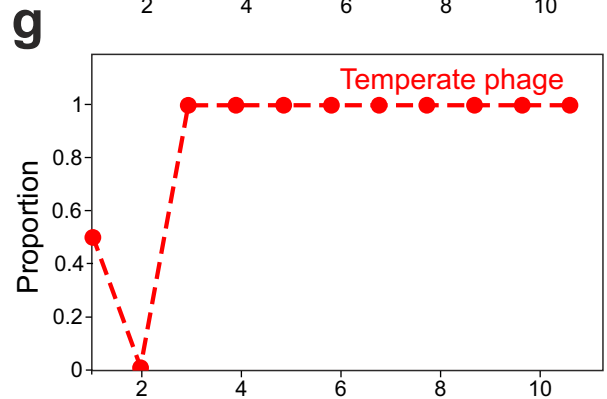
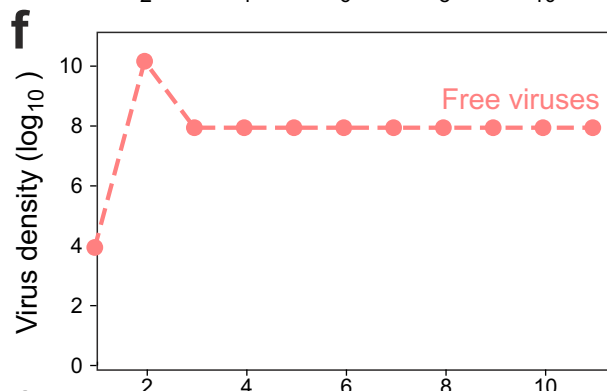
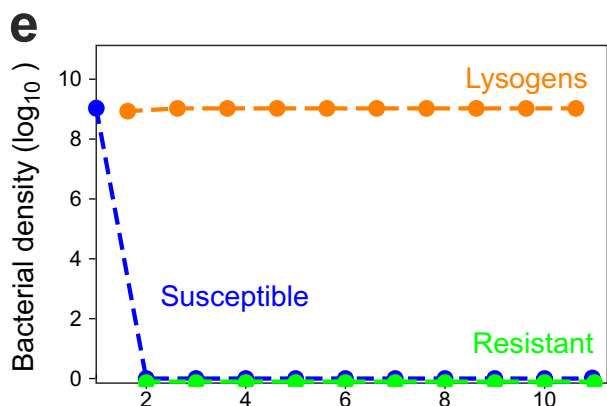
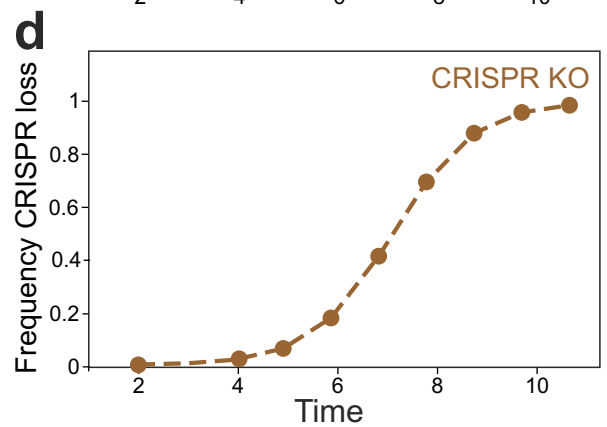
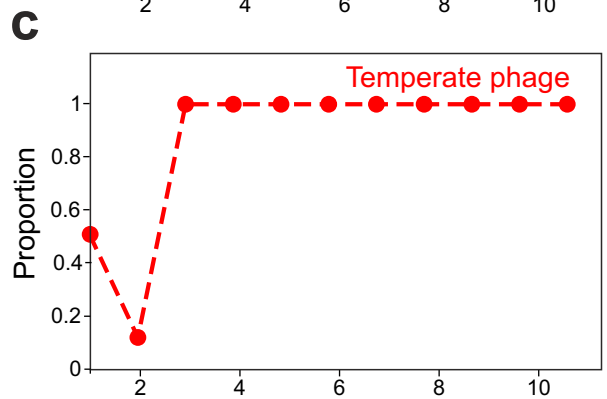
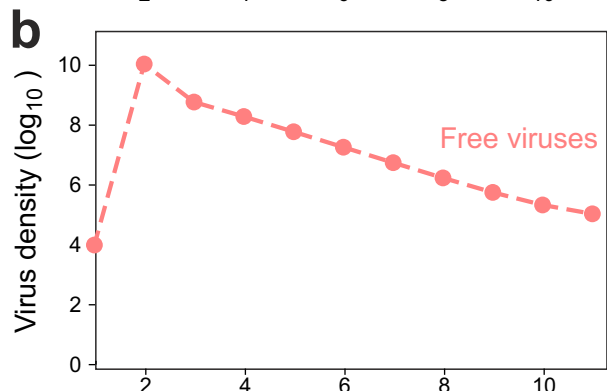
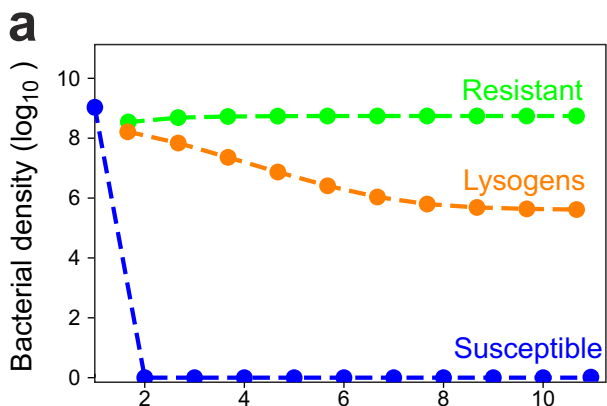


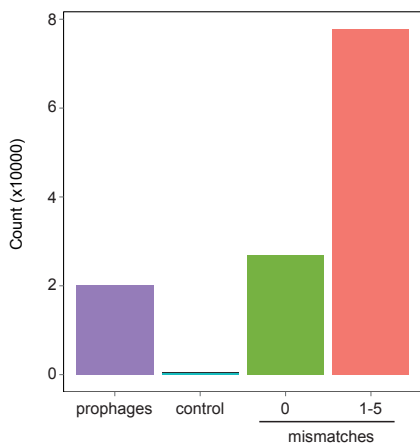
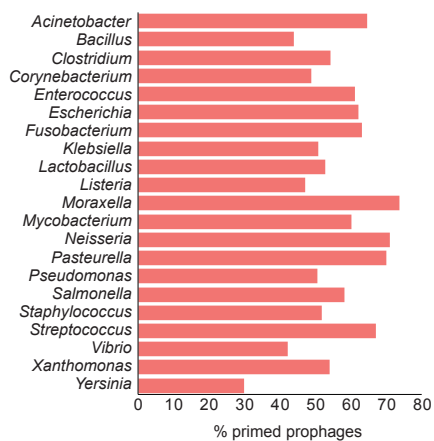
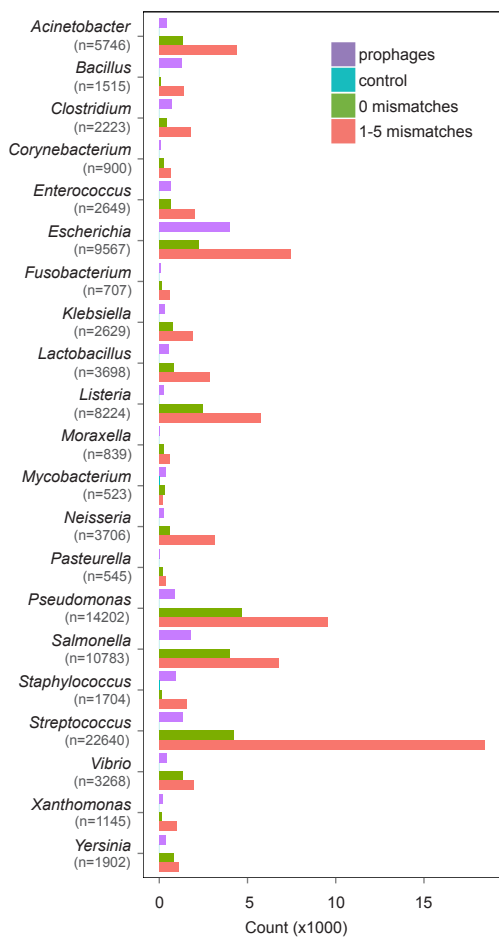
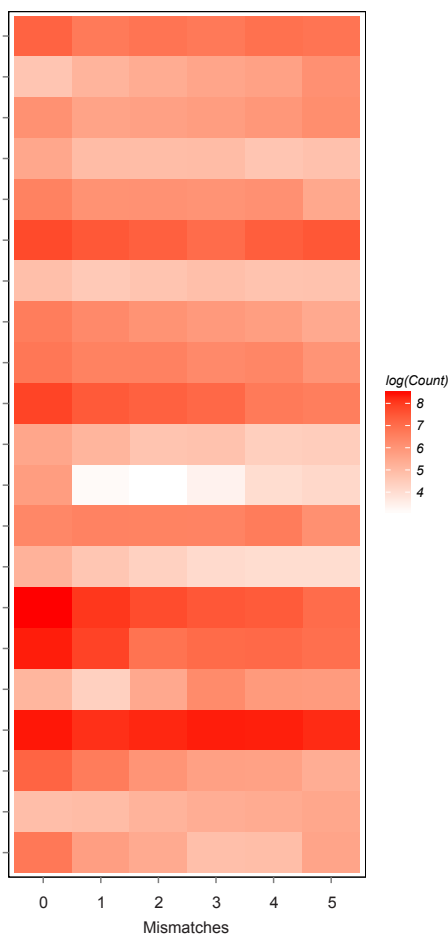
**a****b****Lysogens****c****Prophage Induction****d****DMS3 x DMS3vir**





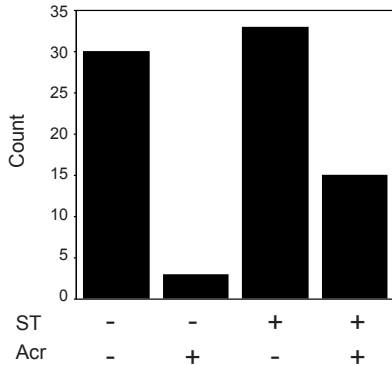
**a****b**



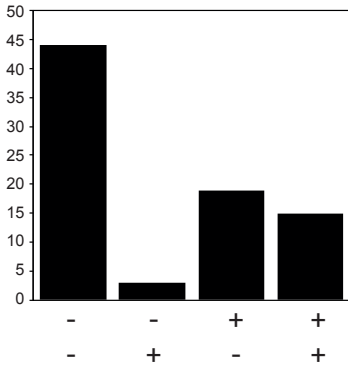
**a****c****b****d**

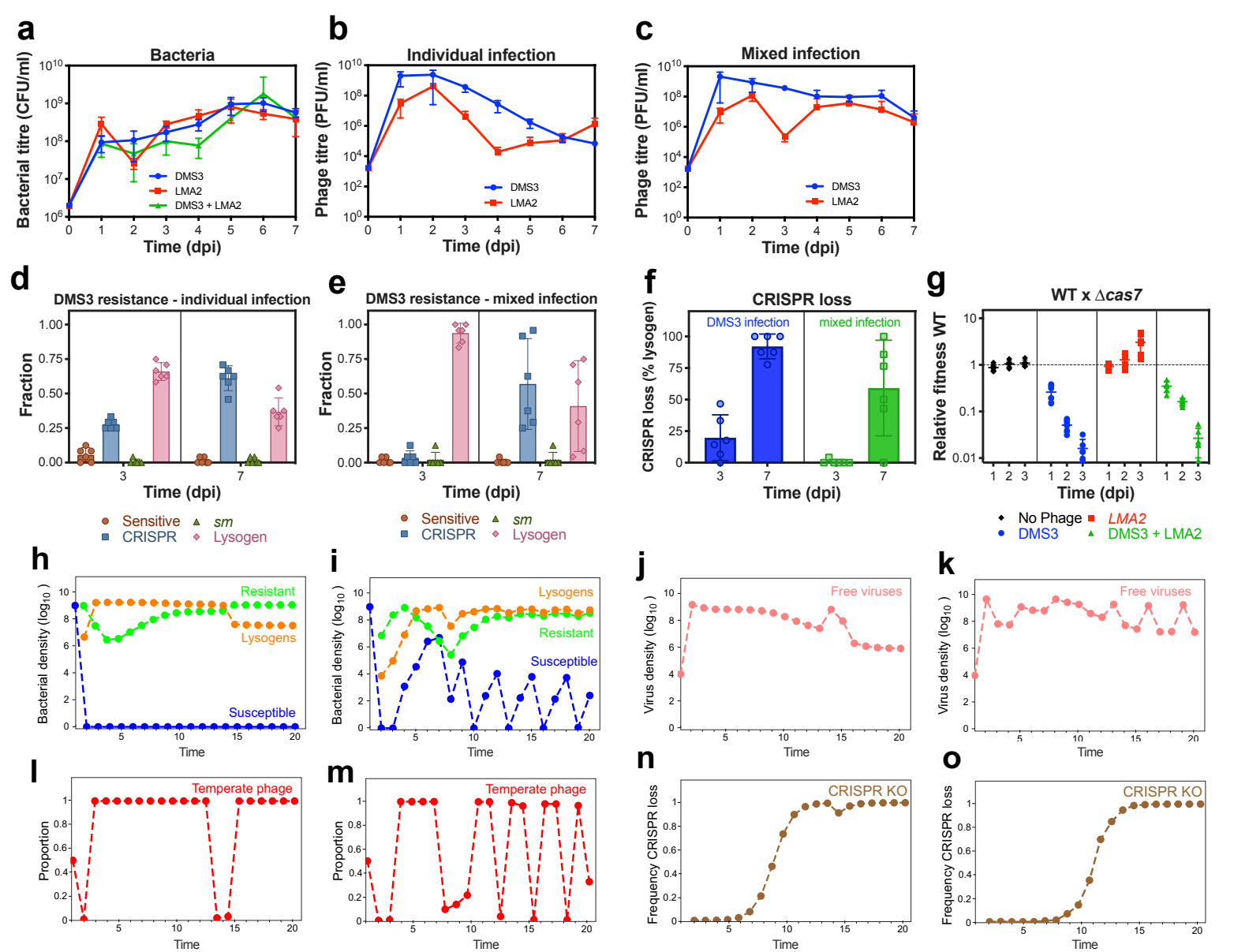
**a**

All self-targets

**b**

Prophage self-targets





1 **Extended Data Table 1 | Genomic deletions and prophage insertion sites in DMS3 late**  
 2 **lysogen clones.**

| Strain                 | Sample name            | Name on ED Fig. 4 | Deleted region |                |                        | Prophage insertion site(s) |  |
|------------------------|------------------------|-------------------|----------------|----------------|------------------------|----------------------------|--|
|                        |                        |                   | Start (bp)     | End (bp)       | Length (bp)            | Position (bp)              | Proportion of mapped hybrid reads <sup>a</sup> |
| PA14<br>WT             | WT117                  | WT_1              | 2,831,115      | 2,938,245      | <b>107,131</b>         | replace deleted region     | 73   |
|                        | WT221                  | WT_2              | 2,879,871      | 2,938,280      | <b>58,410</b>          | replace deleted region     | 44.2   |
|                        | WT3213                 | WT_3              | 2,880,477      | 2,938,285      | <b>57,809</b>          | 3,555,252                  | 42.3   |
|                        | WT4313                 | WT_4              | 2,878,050      | 2,938,509      | <b>60,460</b>          | replace deleted region     | 84   |
|                        |                        |                   |                |                |                        | replace deleted region     | 72.3   |
|                        |                        |                   |                |                |                        | 3,944,997                  | 6.3  |
|                        | WT566 <sup>b</sup>     | -                 | 0              | 0              | <b>0</b>               | 4,067,332                  | 3.8  |
|                        | WT6615                 | WT_5              | 2,812,027      | 2,938,165      | <b>126,139</b>         | 4,453,953                  | 2.5  |
|                        |                        |                   |                |                |                        | replace deleted region     | 42.0   |
|                        |                        |                   |                |                |                        | 3,325,229                  | 49.6   |
| WT7AnneD1              | WT_6                   | 2,743,638         | 2,938,176      | <b>194,539</b> | replace deleted region | 22.6                       |  |
|                        |                        |                   |                |                | 5,214,542              | 28.9                       |  |
|                        |                        |                   |                |                | 5,732,030              | 24.0                       |  |
| WT8AnneD2              | WT_7                   | 2,818,271         | 2,938,290      | <b>120,020</b> | 5,860,538              | 22.6                       |  |
|                        |                        |                   |                |                | 2,335,454              | 24.8                       |  |
|                        |                        |                   |                |                | 2,652,167              | 29.6                       |  |
| replace deleted region | 21.8                   |                   |                |                |                        |                            |  |
| 3,079,052              | 21.3                   |                   |                |                |                        |                            |  |
| PA14<br>$\Delta cas1$  | cas11114               | $\Delta cas1_1$   | 2,918,943      | 2,970,427      | <b>51,485</b>          | 3,079,190                  | 84.3   |
|                        | cas1222                | $\Delta cas1_2$   | 2,706,504      | 2,938,538      | <b>232,035</b>         | replace deleted region     | 90.6   |
|                        | cas1333 <sup>c</sup>   | -                 | 0              | 0              | <b>0</b>               | 4,478,625                  | 2.8  |
|                        | cas14415               | $\Delta cas1_3$   | 2,879,882      | 2,938,523      | <b>58,642</b>          | partial                    | nd   |
|                        |                        |                   |                |                |                        | 2,730,814                  | 44.1   |
|                        | replace deleted region | 46.0              |                |                |                        |                            |  |
|                        | 4,481,869              | 3.1               |                |                |                        |                            |  |
| cas1555 <sup>d</sup>   | -                      | 2,902,848         | 2,938,280      | <b>35,433</b>  | replace deleted region | 78.8                       |  |
| cas16611               | $\Delta cas1_4$        | 2,879,874         | 2,938,285      | <b>58,412</b>  | 2,934,176              | 7.7                        |  |
| replace deleted region | 94.2                   |                   |                |                |                        |                            |  |
| PA14<br>$\Delta cas7$  | cas7114                | $\Delta cas7_1$   | 0              | 0              | <b>0</b>               | 1,120,809                  | 86.7   |
|                        | cas72211               | $\Delta cas7_2$   | 0              | 0              | <b>0</b>               | 410,059                    | 82.9   |
|                        | cas73313               | $\Delta cas7_3$   | 0              | 0              | <b>0</b>               | 5,725,887                  | 74.7   |
|                        | cas7442                | $\Delta cas7_4$   | 0              | 0              | <b>0</b>               | 5,743,045                  | 84.5   |
|                        | cas7554                | -                 | 0              | 0              | <b>0</b>               | 905,180                    | 37.9   |
|                        | cas7669                | -                 | 0              | 0              | <b>0</b>               | 1,667,097                  | 75.0   |

3  
 4 <sup>a</sup>Sum does not reach 100% as a proportion of hybrid reads that mapped PA14 genome did not allow to define  
 5 a potential prophage insertion site.

6 <sup>b</sup>Sample contaminated with a Bacteriophage Insensitive Mutant (BIM) clone; sequencing data not interpretable

7 <sup>c</sup>Only 2607bp of DMS3 DNA (including c-repressor gene) are inserted in bacterial genome at position 5,834,730

8 <sup>d</sup>Mixed population - reads matching the CRISPR locus are still detectable but coverage is very low

## Supplementary Methods:

### Epidemiological modelling of phage dynamics

We develop an epidemiological model to understand the joint dynamics of both virulent and temperate phages in a bacterial host population with a functional CRISPR-Cas system. Initially, a fully susceptible bacterial population is inoculated with  $10^4$  virions. Like in our batch culture experiments, we model the sequential transfer of the community after transferring 1% of the population every day into a new environment with fresh medium. We contrast two different scenarios that differ only in the initial composition of the phage inoculum.

#### Scenario 1: Competition between *related* phages with virulent and temperate life cycles

Following the experiment carried out in our study (Fig. 2a,b) we assume that the phage inoculum is composed of two variants of a single phage species: a temperate strain (the density of this strain is noted  $V_A(t)$ ), and a virulent strain (the density of this strain is noted  $V_V(t)$ ). Both strains can infect susceptible bacteria (the density of susceptible bacteria is noted  $S(t)$ ). Upon infection, three different outcomes are possible:

- (i) Because the two viruses are related, they share the same genome (apart from the gene controlling lysis/lysogeny) and the bacteria can evolve CRISPR resistance against both virus types (the density of resistant bacteria is noted  $R(t)$ ) with a probability of acquisition  $A$ .
- (ii) The phage infection leads to the lysis of the infected cell and produces a burst of  $B$  new virions. The infection by the virulent phage always results in the lysis of the bacteria but the infection by the temperate phage only leads to lysis with a probability  $1 - \phi$ .
- (iii) With probability  $\phi$ , the infection with the temperate phage results in the integration of the virus in the bacterial genome which yields a lysogenic bacterium (the density of lysogenic bacteria is noted  $L(t)$ ).

When lysogens reproduce, they transmit the temperate phage vertically. Note that superinfection inhibition prevents both the temperate and the virulent phages from re-infecting lysogenic bacteria (because both phages are assumed to be related). The prophage in the lysogenic bacterium can reactivate and lyse host cells. Imperfect targeting of the prophage by CRISPR immunity is assumed to yield large induction rates  $\alpha_{CR}$  of the prophage. Lysogenic bacteria can lose the CRISPR locus with a rate  $\mu$  (the density of lysogenic bacteria with an inactive CRISPR is noted  $L_{KO}(t)$ ). Prophages in these lysogenic bacteria are no longer targeted by CRISPR and have a lower induction rate  $\alpha_{KO} < \alpha_{CR}$ .

The above life cycle yields the following set of differential equations (see Supplementary Table 1 for the definition of the parameters of this model):

$$\dot{S}(t) = r(1 - T(t))S(t) - abS(t)V(t) - mS(t) \quad (1)$$

$$\dot{R}(t) = abA(1 - \theta)S(t)V(t) + r(1 - T(t))R(t) - mR(t)$$

$$\begin{aligned} \dot{L}(t) = ab(1 - A(1 - \theta))\phi S(t)V_A(t) + \rho(1 - \mu)(1 - T(t))L(t) \\ - (\alpha_{CR}(1 - \theta) + \alpha_{KO}\theta + m)L(t) \end{aligned}$$

$$\dot{L}_{KO}(t) = \rho(1 - T(t))(\mu L(t) + L_{KO}(t)) - (\alpha_{KO} + m)L_{KO}(t)$$

$$\begin{aligned} \dot{V}_A(t) = ab(1 - A(1 - \theta))(1 - \phi)S(t)V_A(t)B + (\alpha_{CR}(1 - \theta) + \alpha_{KO}\theta)L(t)B \\ + \alpha_{KO}L_{KO}(t)B - (aT(t) + m_V)V_A(t) \end{aligned}$$

$$\dot{V}_V(t) = ab(1 - A(1 - \theta))S(t)V_V(t)B - (aT(t) + m_V)V_V(t)$$

with:  $T(t) = S(t) + R(t) + L(t) + L_{KO}(t)$  and  $V(t) = V_A(t) + V_V(t)$ .

Note that the parameter  $\theta$  refers to the ability for the phage to produce an anti-CRISPR protein (Acr) that prevents both the evolution of CRISPR resistance and immunity against the prophage in lysogenic cells. We plot the dynamics of bacteria and phages across transfers with a wildtype phage (Extended Data Fig. 6a-d) and an Acr-phage (Extended Data Fig. 6e-h). These dynamics are very consistent with the experimental results (compare with Fig. 2a,b). In particular, we recover the short-term increase in the frequency of the virulent phage during the initial epidemic. In addition, we do recover the increase in frequency of bacteria with an inactive CRISPR when the phage does not encode an Acr, but not when the phage encodes an Acr.

## Scenario 2: Competition between unrelated phages with virulent and temperate life cycles

In this second scenario we assume that the virulent and the temperate viruses are unrelated. This has two main consequences. First, CRISPR immunity can be specific to each strain (after the acquisition of a spacer targeting one strain or the other). We thus have to consider three different types of resistant bacteria (see Table S1 for the definition of the parameters of this model):

(1) bacteria resistant to the temperate virus only (the density of these bacteria is noted  $R_A(t)$ );

(2) bacteria resistant to the virulent virus only (the density of these bacteria is noted  $R_V(t)$ );

(3) bacteria resistant to both temperate and virulent viruses after the acquisition to two spacers, one against each virus type (the density of these bacteria is noted  $R_{AV}(t)$ ),

Second, a lysogenic bacterium can be superinfected by the virulent phage.

This yields a modified set of differential equations:

$$\dot{S}(t) = r(1 - T(t))S(t) - abS(t)V(t) - mS(t) \quad (2)$$

$$\dot{R}_A(t) = abA(1 - \theta)S(t)V_A(t) + r(1 - T(t))R_A(t) - (abV_V(t) + m)R_A(t)$$

$$\dot{R}_V(t) = abA(1 - \theta)S(t)V_V(t) + r(1 - T(t))R_V(t) - (abV_A(t) + m)R_V(t)$$

$$\dot{R}_{AV}(t) = abA(1 - \theta)(R_V(t)V_A(t) + R_A(t)V_V(t)) + r(1 - T(t))R_{AV}(t) - mR_{AV}(t)$$



$$\begin{aligned}
\dot{L}(t) &= ab(1 - A(1 - \theta))\phi S(t)V_A(t) + \rho(1 - \mu)(1 - T(t))L(t) \\
&\quad - (\alpha_{CR}(1 - \theta) + \alpha_{KO}\theta + m)L(t) - abL(t)V_V(t) \\
\dot{L}_V(t) &= abA(1 - \theta)L(t)V_V(t) + \rho(1 - \mu)(1 - T(t))L_V(t) \\
&\quad + ab(1 - A(1 - \theta))\phi R_V(t)V_A(t) - (\alpha_{CR}(1 - \theta) + \alpha_{KO}\theta + m)L_V(t) \\
\dot{L}_{KO}(t) &= \rho(1 - T(t))\left(\mu(L(t) + L_V(t)) + L_{KO}(t)\right) - abL_{KO}(t)V_V(t) \\
&\quad - (\alpha_{KO} + m)L_{KO}(t) \\
\dot{V}_A(t) &= ab(1 - A(1 - \theta))(1 - \phi)(S(t) + R_V)V_A(t)B \\
&\quad + ((\alpha_{CR}(1 - \theta) + \alpha_{KO}\theta)L(t) + \alpha_{KO}L_{KO}(t))B - (aT(t) + m_V)V_A(t) \\
\dot{V}_V(t) &= ab\left((1 - A(1 - \theta))(S(t) + R_A + L(t)) + L_{KO}(t)\right)V_V(t)B - (aT(t) \\
&\quad + m_V)V_V(t)
\end{aligned}$$

$$\text{with: } T(t) = S(t) + \underbrace{R_A(t) + R_V(t) + R_{AV}(t)}_{R_T(t)} + \underbrace{L(t) + L_V(t) + L_{KO}(t)}_{L_T(t)}.$$

This scenario yields more complex dynamics because it can maintain transient polymorphism in both bacteria and phage populations through negative frequency dependence (Extended Data Fig. 9h, j, l, n). The presence of a virulent phage in the population maintains the fitness benefit associated with carrying an active CRISPR-Cas system (note how the selection for CRISPR is associated with the high frequency of the virulent phage). Yet, after the spread of resistant bacteria, the virulent phage is outcompeted by the temperate phage and, among the lysogens, there is selection for the loss of the CRISPR-Cas system.

To match the biology of our experimental system we also modeled a situation where CRISPR-Cas cannot acquire immunity against the virulent phage. Yet, we allow the evolution of costly surface mutations that block the infection by the virulent phage. This yields the following set of differential equations (where the subscript  $V$  refers to surface mutation blocking the virulent phage):

$$\begin{aligned}
\dot{S}(t) &= r(1 - \mu_R)(1 - T(t))S(t) - abS(t)V(t) - mS(t) & (3) \\
\dot{R}_A(t) &= abA(1 - \theta)S(t)V_A(t) + r(1 - \mu_R)(1 - T(t))R_A(t) - (abV_V(t) + m)R_A(t) \\
\dot{R}_V(t) &= r\mu_R(1 - T(t))S(t) + r(1 - c)(1 - T(t))R_V(t) - (abV_A(t) + m)R_V(t) \\
\dot{R}_{AV}(t) &= abA(1 - \theta)R_V(t)V_A(t) + r\mu_R(1 - T(t))R_A(t) \\
&\quad + r(1 - c)(1 - T(t))R_{AV}(t) - mR_{AV}(t) \\
\dot{L}(t) &= ab(1 - A(1 - \theta))\phi S(t)V_A(t) + \rho(1 - \mu)(1 - \mu_R)(1 - T(t))L(t) \\
&\quad - (\alpha_{CR}(1 - \theta) + \alpha_{KO}\theta + m)L(t) - abL(t)V_V(t) \\
\dot{L}_V(t) &= \rho(1 - \mu)\mu_R(1 - T(t))L(t) + \rho(1 - \mu)(1 - c)(1 - T(t))L_V(t) \\
&\quad + ab(1 - A(1 - \theta))\phi R_V(t)V_A(t) - (\alpha_{CR}(1 - \theta) + \alpha_{KO}\theta + m)L_V(t)
\end{aligned}$$

$$\begin{aligned}
\dot{L}_{KO}(t) &= \rho(1 - \mu_R)(1 - T(t))(\mu L(t) + L_{KO}(t)) - abL_{KO}(t)V_V(t) \\
&\quad - (\alpha_{KO} + m)L_{KO}(t) \\
\dot{L}_{KO,V}(t) &= \rho(1 - T(t))(\mu_R L_{KO}(t) + \mu(1 - c)L_V(t) + (1 - c)L_{KO,V}(t)) \\
&\quad - (\alpha_{KO} + m)L_{KO,V}(t) \\
\dot{V}_A(t) &= ab(1 - A(1 - \theta))(1 - \phi)(S(t) + R_V)V_A(t)B \\
&\quad + \left( (\alpha_{CR}(1 - \theta) + \alpha_{KO}\theta)(L(t) + L_V(t)) \right. \\
&\quad \left. + \alpha_{KO}(L_{KO}(t) + L_{KO,V}(t)) \right) B - (aT(t) + m_V)V_A(t) \\
\dot{V}_V(t) &= ab \left( (1 - A(1 - \theta))(S(t) + R_A + L(t)) + L_{KO}(t) \right) V_V(t)B - (aT(t) \\
&\quad + m_V)V_V(t)
\end{aligned}$$

We observe very similar dynamics as in the previous scenario: the spread of multi-resistant hosts, the fixation of the temperate phage and the loss of CRISPR. However, when the cost of resistance against the virulent phage is high, the virulent phage can be maintained in the population because a polymorphism is maintained between susceptible and resistant bacteria by negative frequency dependent selection (Extended Data Fig. 9i, k, m, o). Note however, that the presence of the virulent phage does not maintain CRISPR because in this scenario, bacteria do not rely on CRISPR immunity to resist infection by the virulent phage.

**Overall conclusion of modelling:** Our model tracks both the evolution of phages (life cycle, evolution of *acr*) and bacteria (evolution of CRISPR immunity or surface mutations). The good fit between the output of the model (Extended Data Fig. 6 and 9h-o) and our experimental results (Fig. 2 and Extended Data Fig. 9a-g, respectively) supports the hypothesis that the cost of virulence is driving the evolution of phage life cycle (lytic versus lysogenic life cycle) and the cost of auto-immunity in lysogenic bacteria is driving the evolutionary loss of CRISPR-Cas in bacteria. Besides, the model allows to explore other scenarios such as the competition between unrelated viruses. Most scenarios lead to the evolutionary loss of CRISPR-Cas in lysogens. Indeed, in our model, once resistance against virulent phage is present (i.e. CRISPR-based or surface mutant), there is no need to invest in immunity because it carries high fitness costs in lysogenic bacteria.

Note that our experiments (and our model) describe the evolution of a closed system. More complex scenarios, for example where a bacterial population is constantly exposed to new unrelated virulent phages (e.g. immigrating from other locations), remain to be explored.

**Supplementary Table 1: Parameters of the model with default values**

| Parameter     | Definition   | Default value                                     |
|---------------|--|---|
| $r$           | Growth rate of uninfected cells  | $0.7 h^{-1}$                                      |
| $\rho$        | Growth rate of infected cells  | $0.7 h^{-1}$                                      |
| $K$           | Carrying capacity  | $10^9 \text{ cells}$                              |
| $B$           | Burst size   | $50 \text{ virion. cell}^{-1}$                    |
| $a$           | Adsorption constant  | $5 \times 10^{-10} h^{-1} \cdot \text{cell}^{-1}$ |
| $b$           | Probability of fusion after adsorption   | $10^{-1}$   |
| $\phi$        | Probability of genome integration  | 0.5   |
| $A$           | Probability of acquisition of a new spacer targeting the phage                               | $10^{-4}$   |
| $\theta$      | Efficacy of CRISPR inhibition by Acr   | 0 (wildtype phage)<br>1 (Acr-phage)               |
| $\alpha_{CR}$ | Induction rate of the prophage when the CRISPR immunity targets the prophage                 | $5 \cdot 10^{-2} h^{-1}$                          |
| $\alpha_{KO}$ | Induction rate of the prophage when the CRISPR immunity does not target the prophage         | $10^{-3} h^{-1}$                                  |
| $m$           | Mortality rate of bacteria   | $0 h^{-1}$  |
| $m_V$         | Mortality rate of virions  | $0 h^{-1}$  |
| $\mu$         | Mutation towards CRISPR KO   | $10^{-4}$   |
| $\mu_R$       | Mutation towards <i>sm</i> resistance against the lytic virus (see equation (3))             | $10^{-4}$   |
| $c$           | Fitness cost associated with <i>sm</i> resistance against the lytic virus (see equation (3)) | 0.5   |

## Bioinformatic analysis of widespread priming off temperate phages

The maladaptation hypothesis predicts that bacteria that continue to benefit from prophages, yet contain mismatched spacers against the prophage, would be under pressure to reduce or lose CRISPR-Cas function. Specifically, bacteria with spacers having near matches within the prophage would be maladapted (e.g. PA14 CRISPR2 spacer 1/DMS3) as self-targeting or self-priming could occur. If this were widespread, we predict that (i) spacers matching prophages would be common within the pan-spacer repertoire for a genus (ii) genomes with self-targeting or self-priming spacers would either have *acr(s)*, or that the CRISPR-Cas system would be non-functional.

### ***(i) Spacers matching temperate phages are common***

To test if it is common for bacteria to possess pre-existing spacers that may promote priming off temperate phages, we tested a set of all spacers from 171,361 bacterial genomes against a database of prophage sequences<sup>21</sup>. Genomes from RefSeq 93 (n=136,507) were supplemented with Genbank genomes absent from RefSeq (giving a total of 171,361). CRISPR arrays were identified using CRISPRDetect<sup>34</sup>; 1,239,937 spacers were collected (spacers of atypical size were removed as potential artefacts) and identified by the genomic contig, position and species. A set of prophage sequences from the PHAST<sup>21</sup> database were de-replicated and split into 133 genera from 6570 complete genomes (total n=19,996). For each bacterial genus in which prophages were found, we searched for prophage targets using a non-redundant set of spacers (generated by CD-HIT-dup, default parameters) from species within the same genus (using BLASTN; blastn-short, e-value cut-off=0.001, DB-size=10000, word-size=7, gap-open penalty=10, gap-extension=-2, mismatch=-1, match reward=1). A total of 85,931 hits with 0-5 mismatches were identified within all genera (e.g. from any *Streptococcus* spacer against any *Streptococcus* prophage there were 10,850 hits).

Compared with a negative control, where the non-redundant prophage database was hexanucleotide shuffled 10 times to reveal the number of random hits (276 +/- 30), there was a significant increase in within-genus prophage hits from spacers with either 0 mismatches or 1-5 mismatches (Extended Data Fig. 7a). Next, the distributions of mismatch frequencies were computed per genus for those with over 500 within genus spacer-phage matches (0-5 mismatches). All genera had significantly more matches compared with a shuffled dataset (Extended Data Fig. 7b). The distributions of number of mismatches differed between genera. For example, *Pseudomonas* spp. and *Mycobacterium* spp. had many exact matches but other genera displayed more evenly distributed mismatch frequencies (Extended Data Fig. 7c). In conclusion, it is common for many bacterial genera to contain pre-existing spacers that are likely to either provide interference or priming off invading temperate phage genomes. These data support maladaptation hypothesis of CRISPR-Cas against temperate phages.

### ***(ii) Self-targeted and self-primed genomes are enriched for Acr(s).***

Our experimental data indicated that the maladaptive effects of CRISPR-Cas against temperate phages can be countered through Acr proteins or be tolerated due to CRISPR-Cas inactivation or

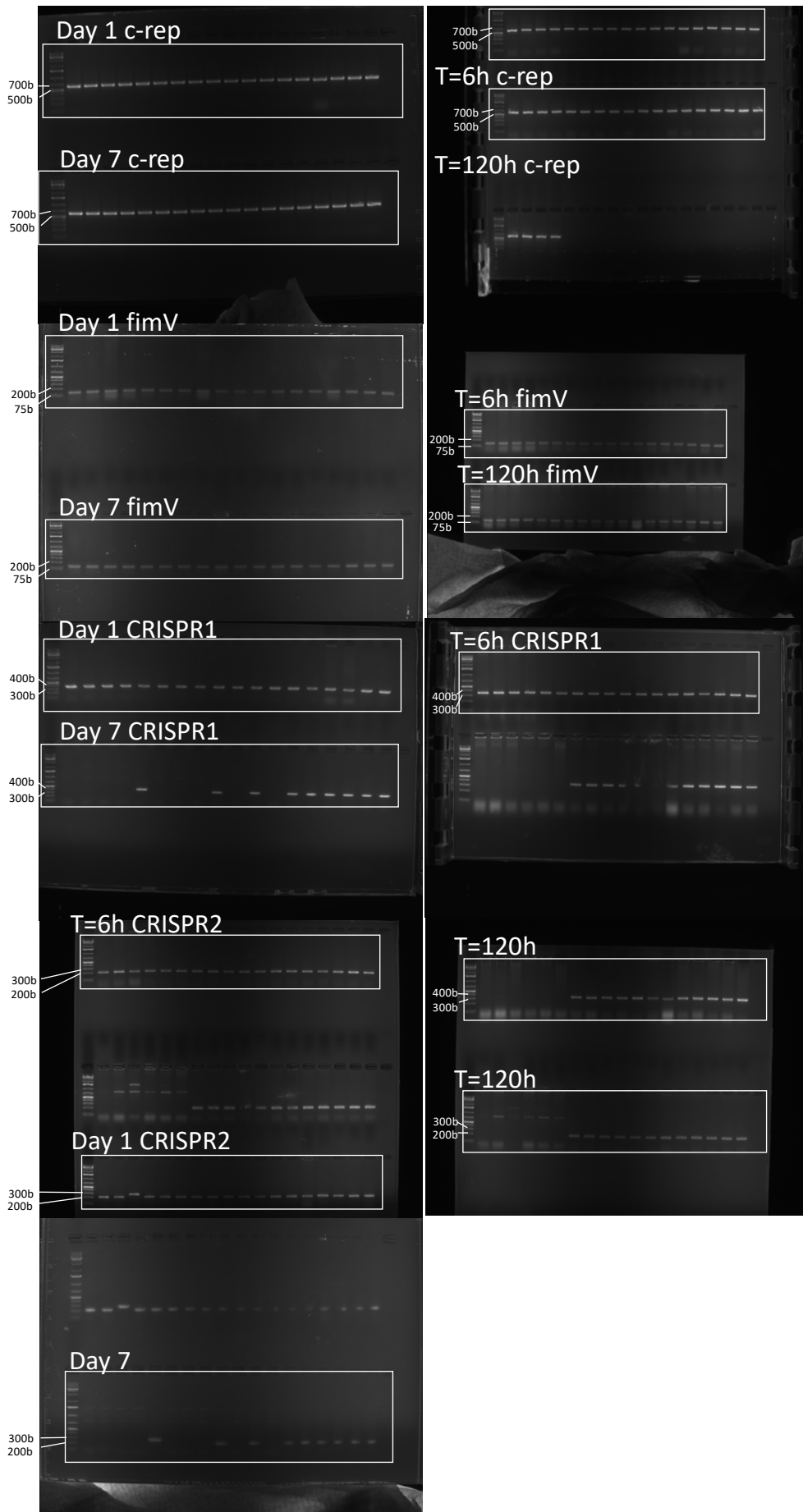
loss. First, we sought to further test this finding by searching sequenced bacterial genomes for self-targeting or self-priming and whether this correlated with the presence of *acr* genes. Strains of *P. aeruginosa* provide a good test set since there are many sequenced isolates, several *acr* genes have been identified, and prophages are common. In addition, the main CRISPR-Cas types are I-E and I-F, where priming has been demonstrated experimentally.

To test if self-targeting leads to increased Acr presence, CRISPR arrays were identified using CRISPRDetect in 98 of 168 *P. aeruginosa* genomes. CRISPRCasFinder<sup>35</sup> was used to assign whether *cas* gene sets were complete and only those strains analysed further. These strains were characterized as either containing no self-targets or self-matches using the self-targeting spacer searcher (STSS)<sup>36</sup>, with the BLASTN parameters modified to permit up to 5 mismatches (0-5). Next, *acr* genes were identified by building hmm using proteins with >40% identity to the set of known *acr* genes from STSS. We observed a statistically significant enrichment for increased frequencies of *acr* genes in the presence of self-targeting spacers, in support of our experimental data (Extended Data Fig. 8a). An even stronger association between *acr* genes and self-matches was observed when the analysis considered self-targets within prophages (identified using PHASTER<sup>37</sup>) (Extended Data Fig. 8b).

Note that further analysis of this dataset did not reveal increased frequencies of *cas* gene deletions from genomes with priming spacers against prophages (data not shown). This is likely explained by (i) the limited number of *P. aeruginosa* genomes that match our search criteria, (ii) genetic linkage that causes deletions to typically encompass both *cas* genes and CRISPR arrays (Extended Data Fig. 4c-e), and (iii) presence of unidentified *acr* genes in prophage genomes that are not detected by our search algorithm due to sequence divergence from currently described *acr* genes.

## References :

21. Zhou, Y., Liang, Y., Lynch, K. H., Dennis, J. J. & Wishart, D. S. PHAST: a fast phage search tool. *Nucleic Acids Res.* **39**, W347-352 (2011).
34. Biswas, A., Staals, R. H. J., Morales, S. E., Fineran, P. C. & Brown, C. M. CRISPRDetect: A flexible algorithm to define CRISPR arrays. *BMC Genomics* **17**, 356 (2016).
35. Couvin, D. *et al.* CRISPRCasFinder, an update of CRISPRFinder, includes a portable version, enhanced performance and integrates search for Cas proteins. *Nucleic Acids Res.* **46**, W246–W251 (2018).
36. Watters, K. E., Fellmann, C., Bai, H. B., Ren, S. M. & Doudna, J. A. Systematic discovery of natural CRISPR-Cas12a inhibitors. *Science* **362**, 236–239 (2018).
37. Arndt, D. *et al.* PHASTER: a better, faster version of the PHAST phage search tool. *Nucleic Acids Res.* **44**, W16–W21 (2016).



**Supplementary Figure 1** : Source data images for PCR amplification results presented in Figure 4a-d. Cropped areas are indicated by white boxes.